Industrial Applications

- Electronics
  - Gate oxide films for LSI
  - Thin films for storage devices, etc
- materials
  - Safety tire, fibers
  - Metal coats, etc
- Energy & environments
  - Detection of metals in human hair
  - battery

JASRI Satoshi Komiya

Industrial Applications of SR

Characterization of materials

–Structure, Chemical state, Contamination, etc.

thin films for electronic devices;LSI, HDD, lasers

metals、polymers, batteries,catalyses

–high **brilliant** source, x-ray ; big machine

Production technology

–lithography, photo-assisted etching or deposition

–high **flux** source, ultra-violet-soft x-ray;

small machine

Industrial Applications

Synchrotron radiation

electronics

- Films for ULSI, semiconductors
- HDD, DVD
- Semiconductor laser

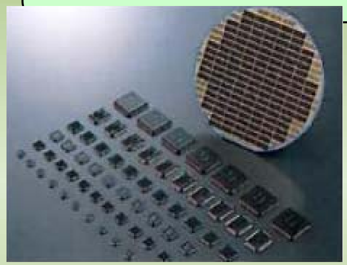

Metals & Soft materials

- Steel & Coats on steel
- Al included bubbles

- Tires
- Fibers

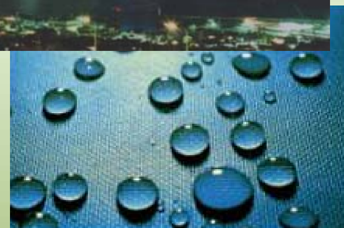

Energy & Environment

- Batteries: fuel cell & Li-ion
- Analysis of contamination elements
- Catalysts for environment

Others

- Building materials
- Catalysis
- Insects

Life science

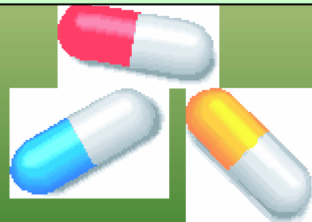

- medicine

CMOS Structure

key points for R&D:gate & lines

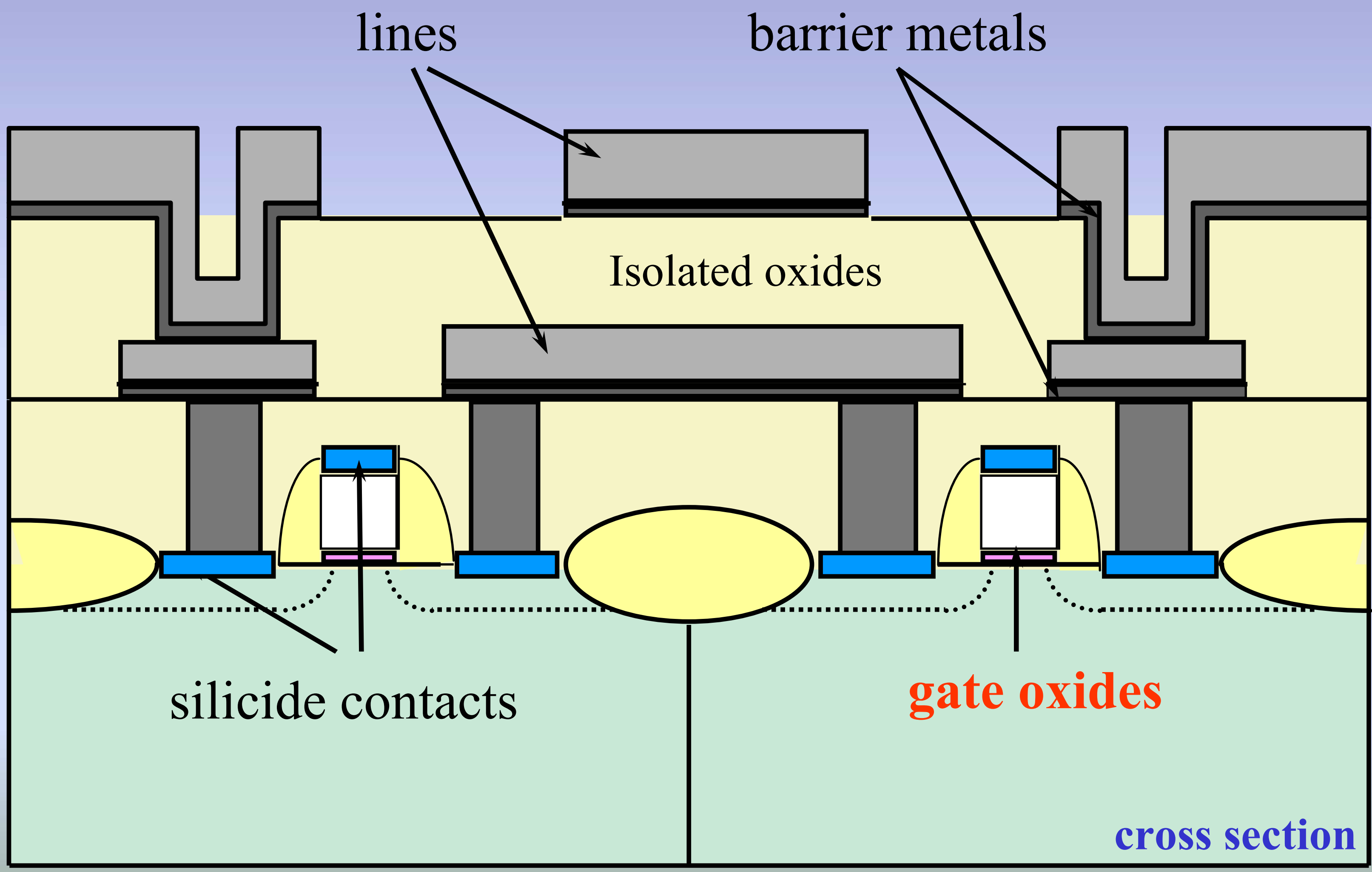

Grazing incident x-ray reflection and diffraction

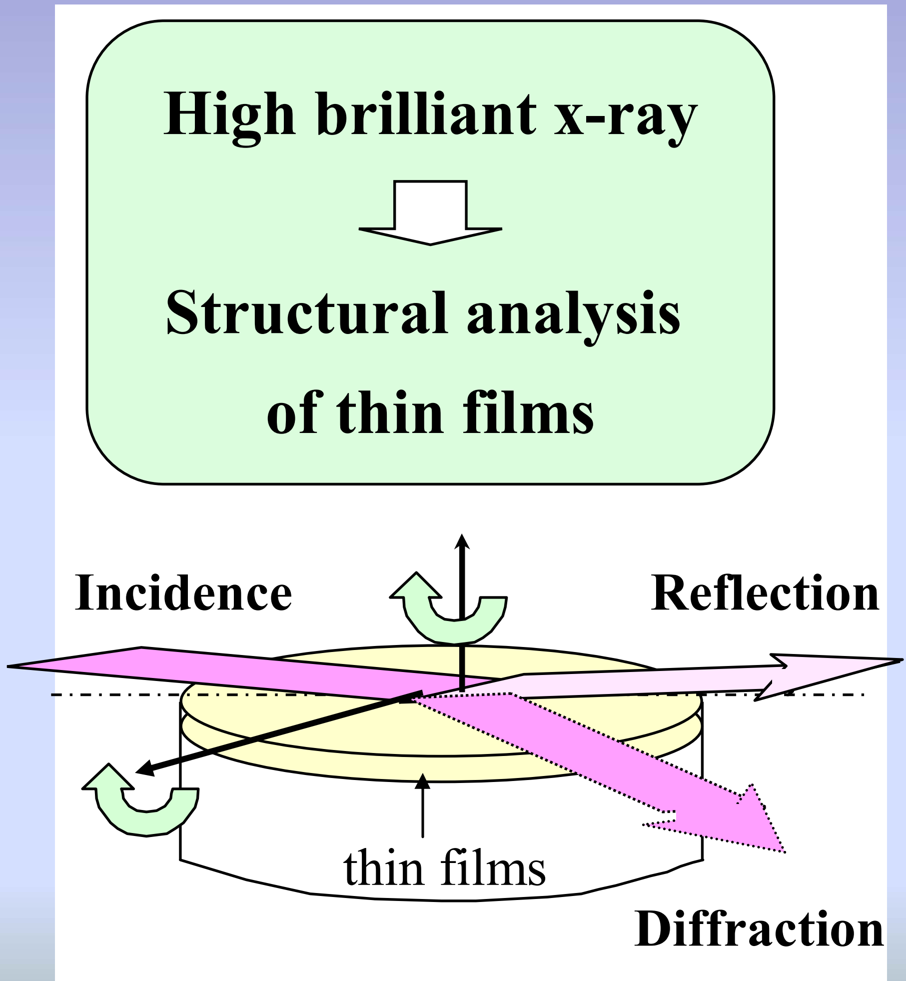

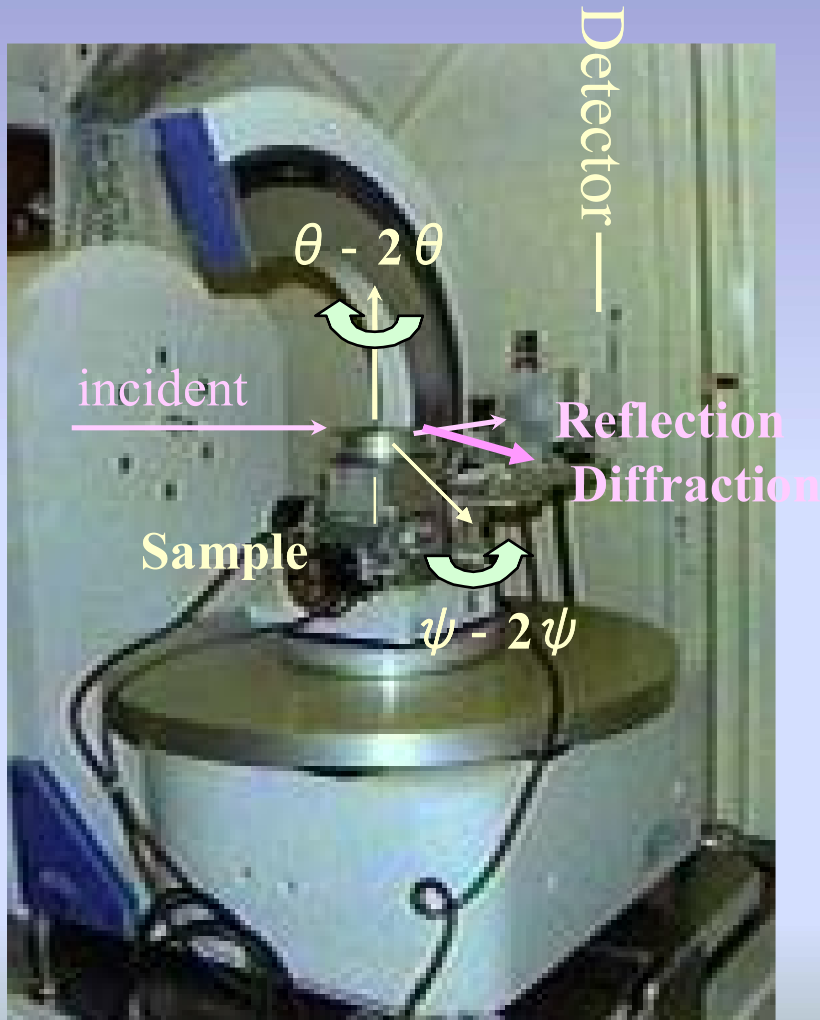

X-ray reflectivity analysis

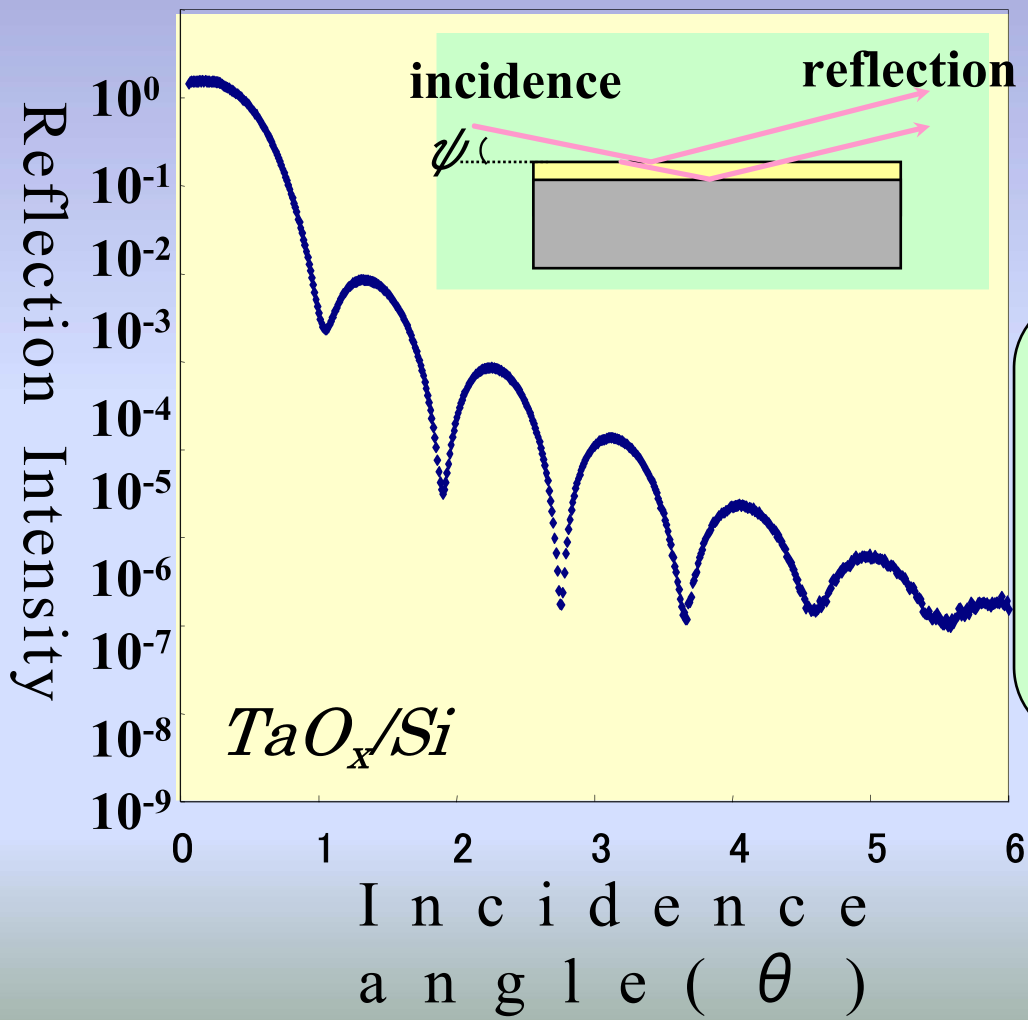

Information obtained by reflectivity analysis

Reflectivity		Information
•Period	⇨	Thickness
•Amplitude	⇨	Density
•Damping	⇨	Roughness

X-ray reflectivity profiles of oxide films on silicon substrates

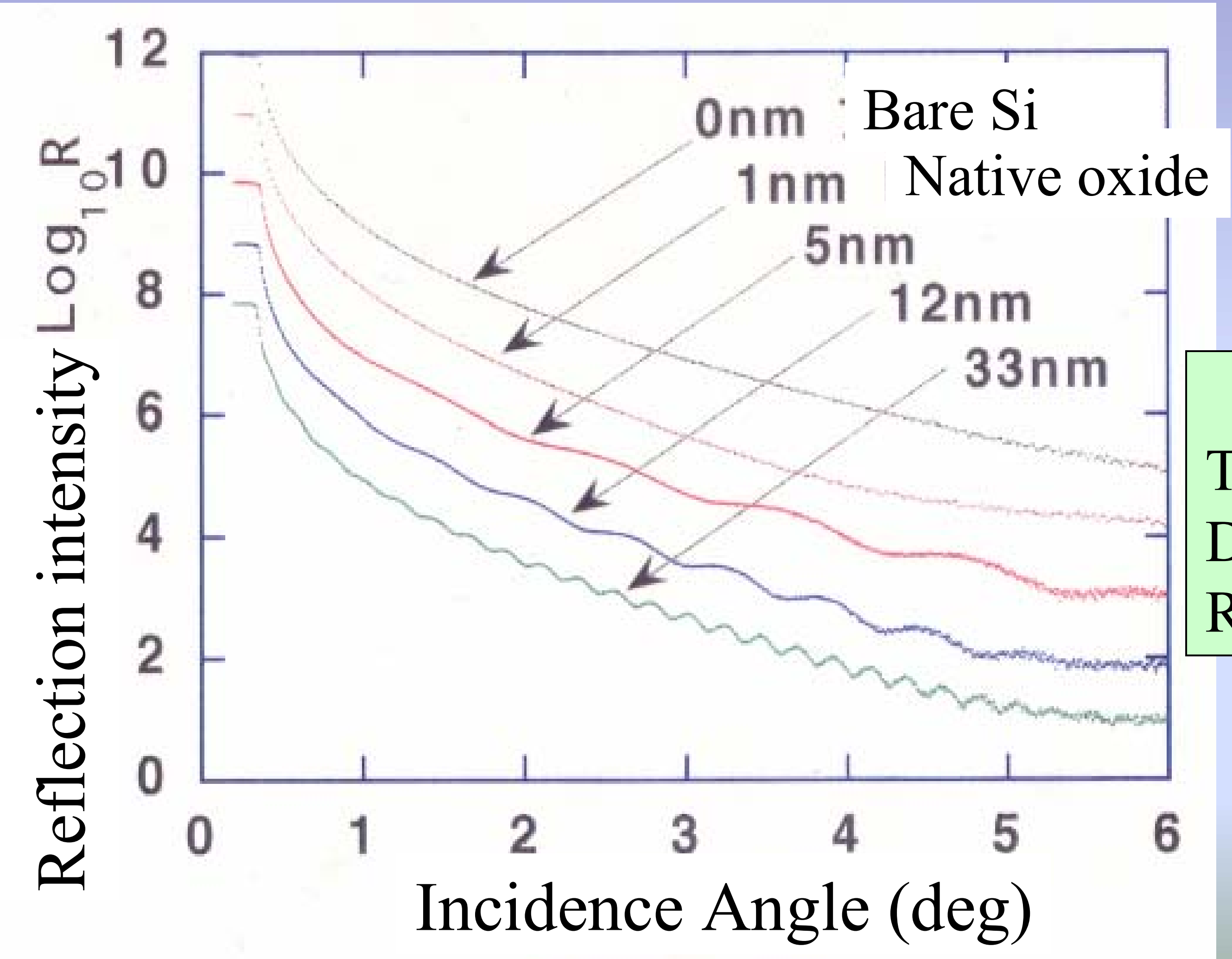

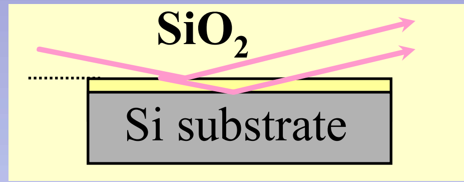

Accuracy

Thickness : 0.01nm

Density : 0.01g/cm^3

Roughness : 0.02nm

X-ray reflectivity profile and interference components (calculation)

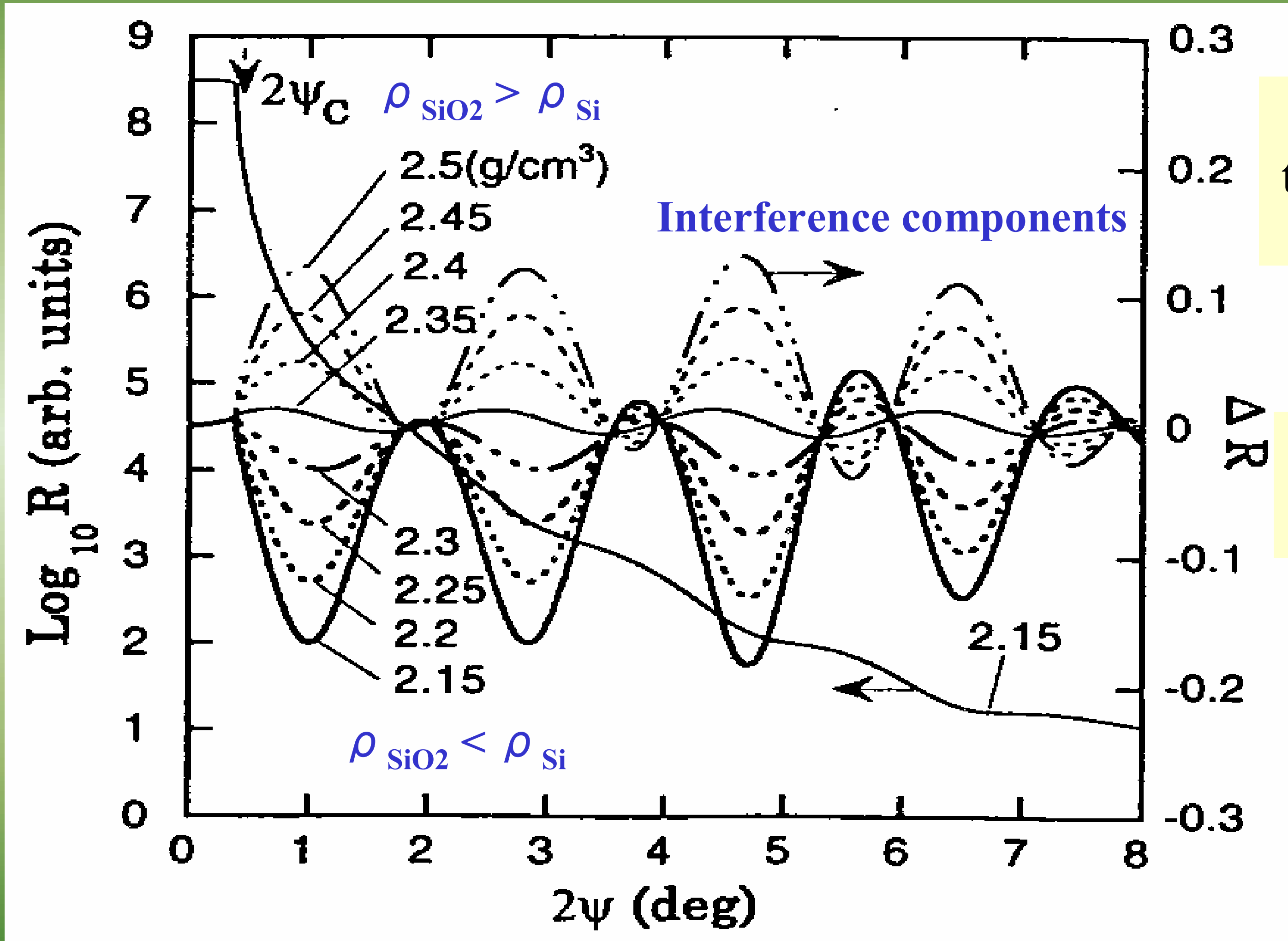

SiO_2 on Si
thickness : 4nm
ρ_{Si}=2.33 g/cm^3

$\Delta R = \log_{10}(R/R_{ave})$
R_{ave}:reference

Subtraction technique of the interference component derive easy analysis.

Analysis with the interference component

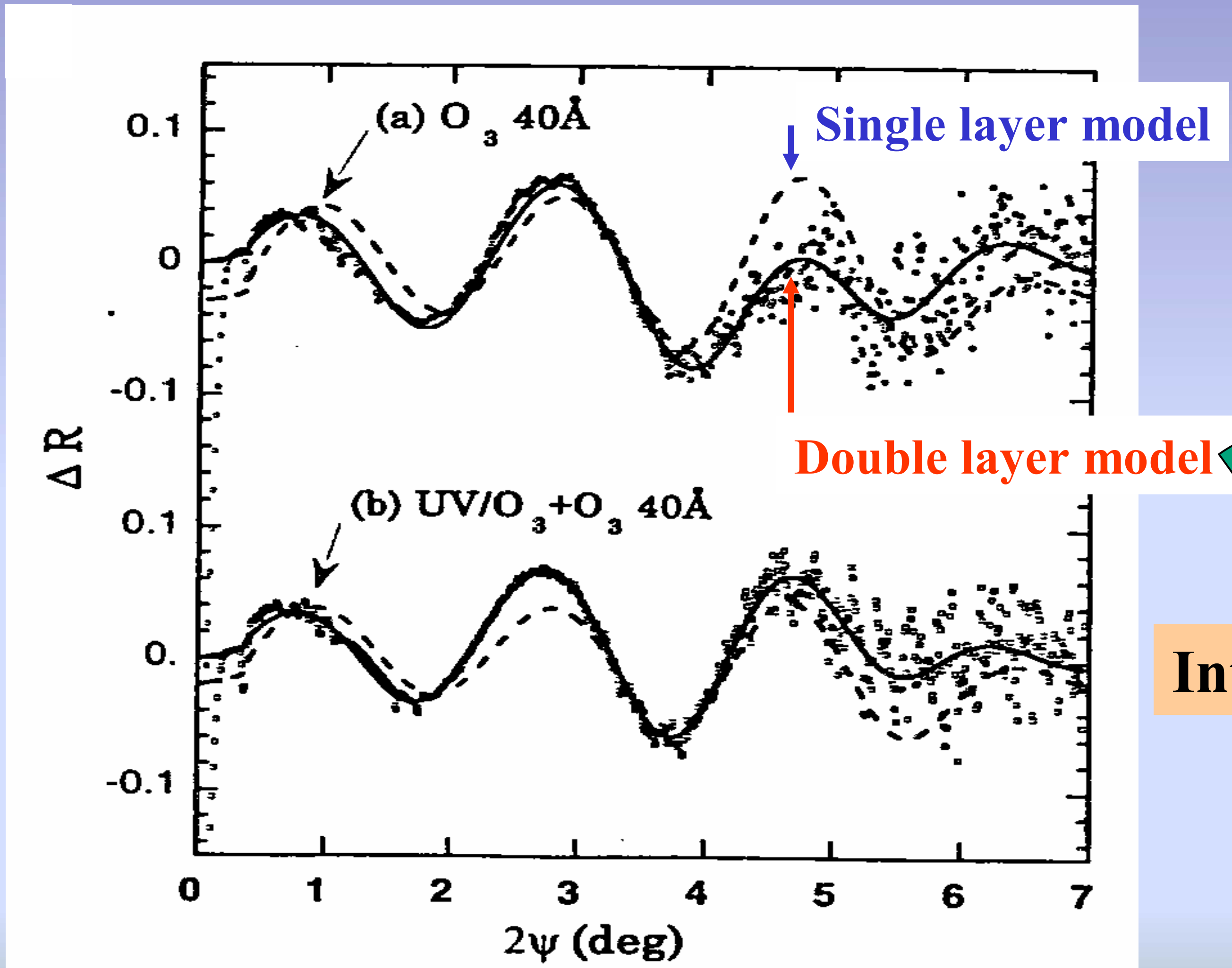

Interfacial layer

4nm thin SiO_2 on Si fabricated by thermal oxidation

Generation of high dense interfacial layer on thermal oxidation process

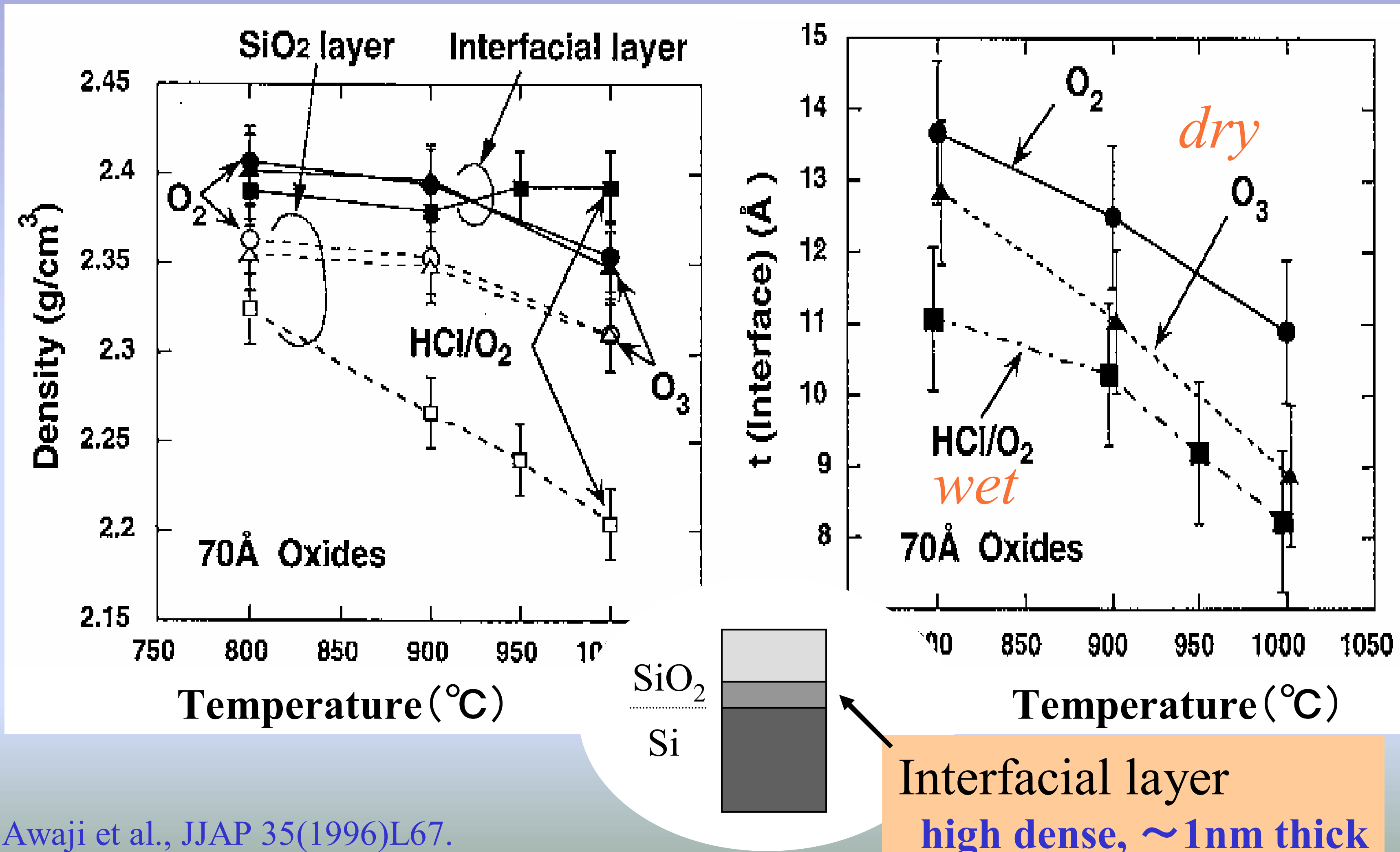

Interfacial layer
high dense, ~1nm thick

N.Awaji et al., JJAP 35(1996)L67.

Development of measurement technique

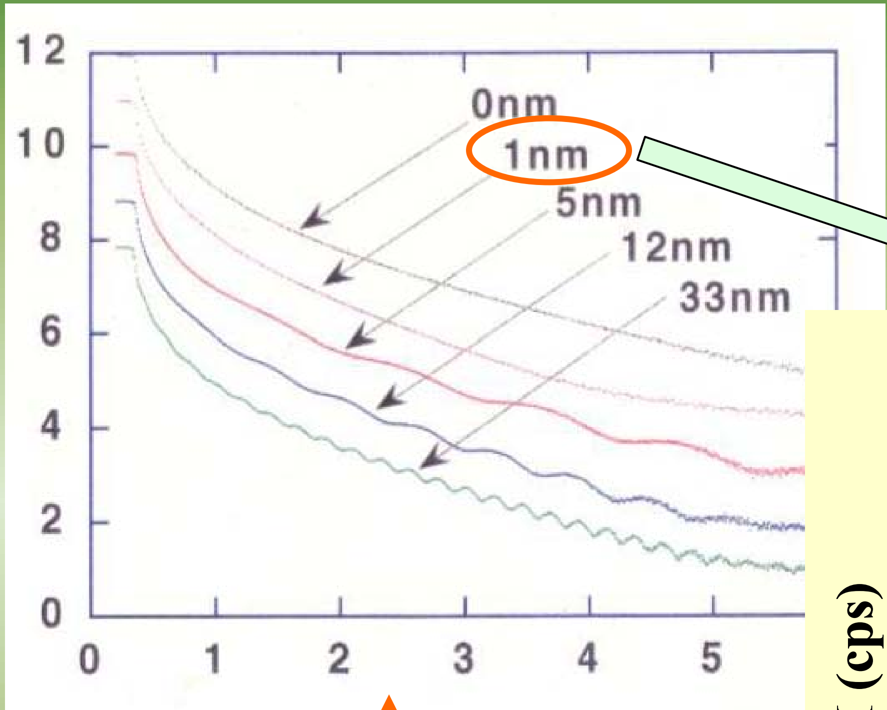

Accurate evaluation of ultra-thin films

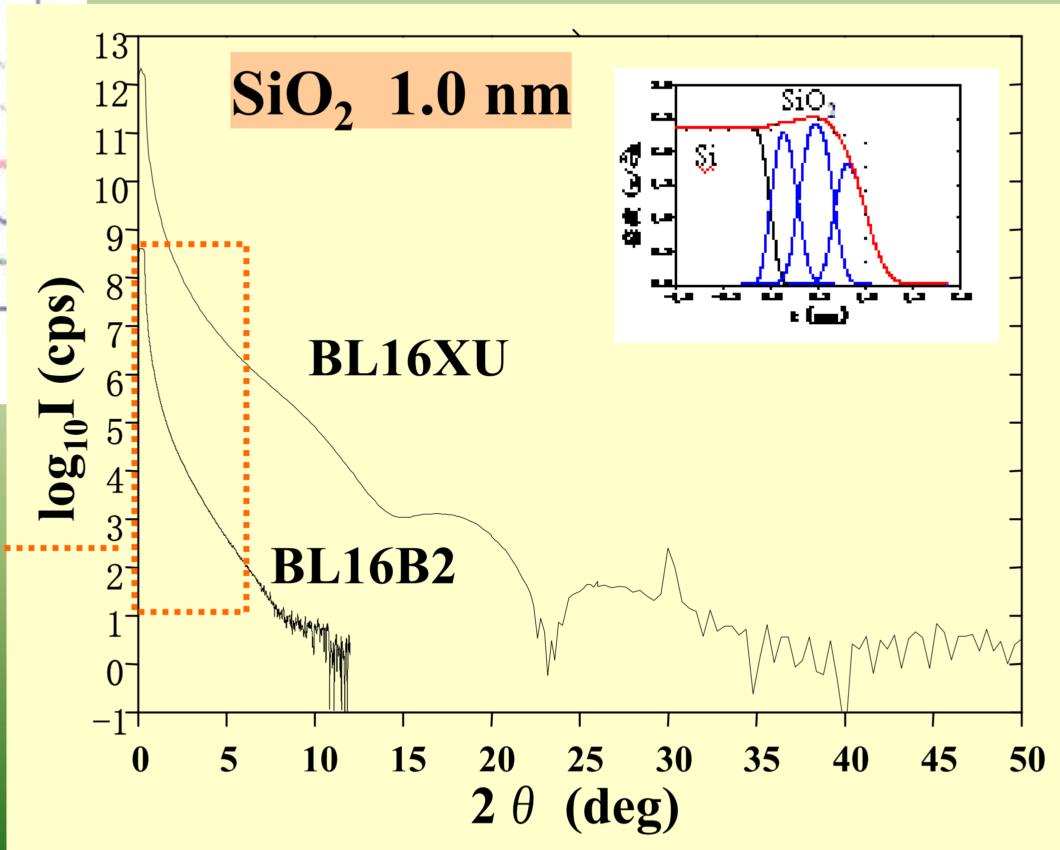

Same region

BL16XU:undulator beamline
BL16B2:bending magnet beamline

N.Awaji in Fujitsu Labs.

Observation of crystalline SiO_2 in thermal oxides

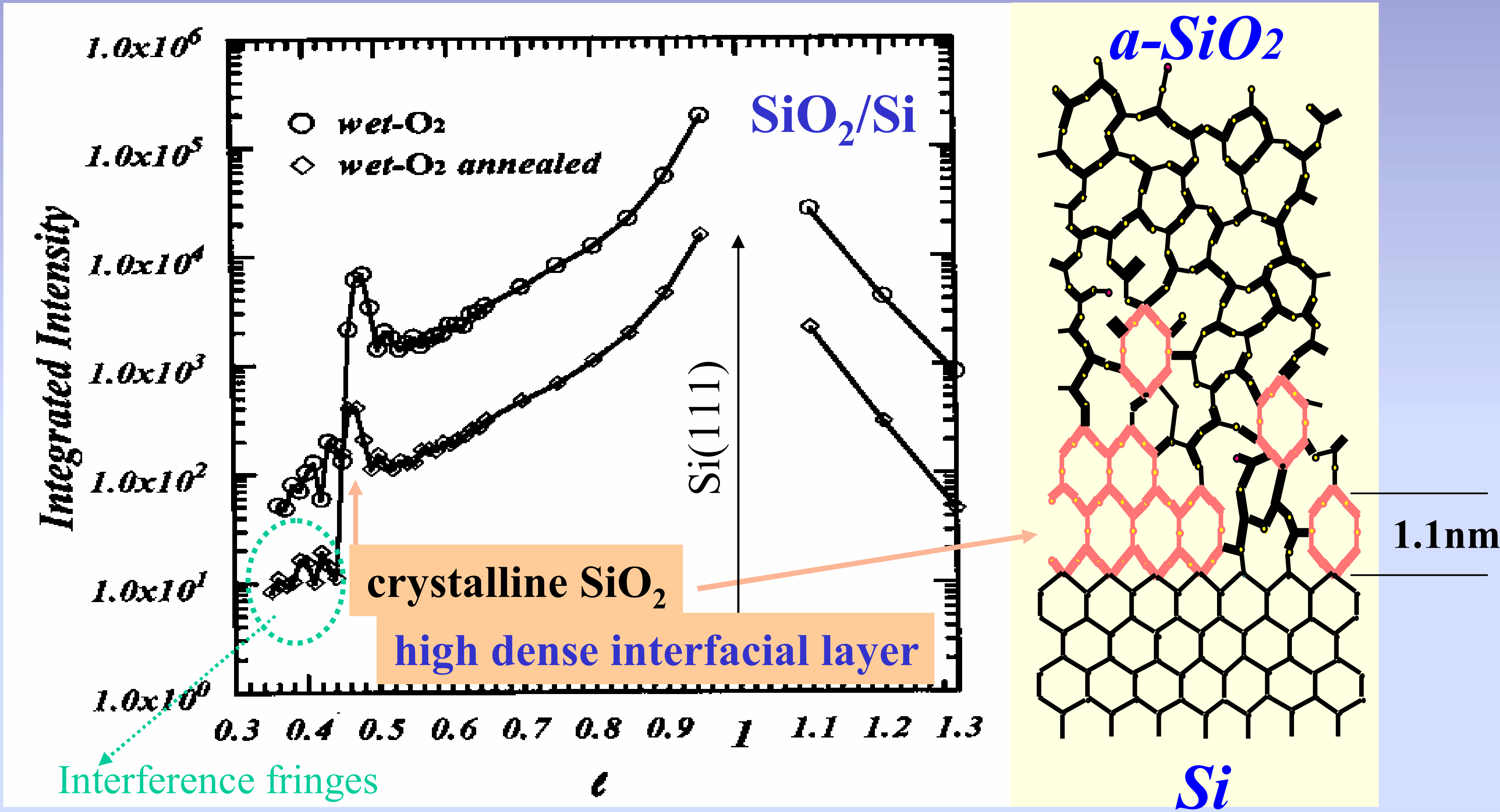

X-ray Crystal Truncation Rod Scattering

I.Takahashi et al., Physica B245(1998) 306.

In-situ observation of CTR scattering during thermal oxidation

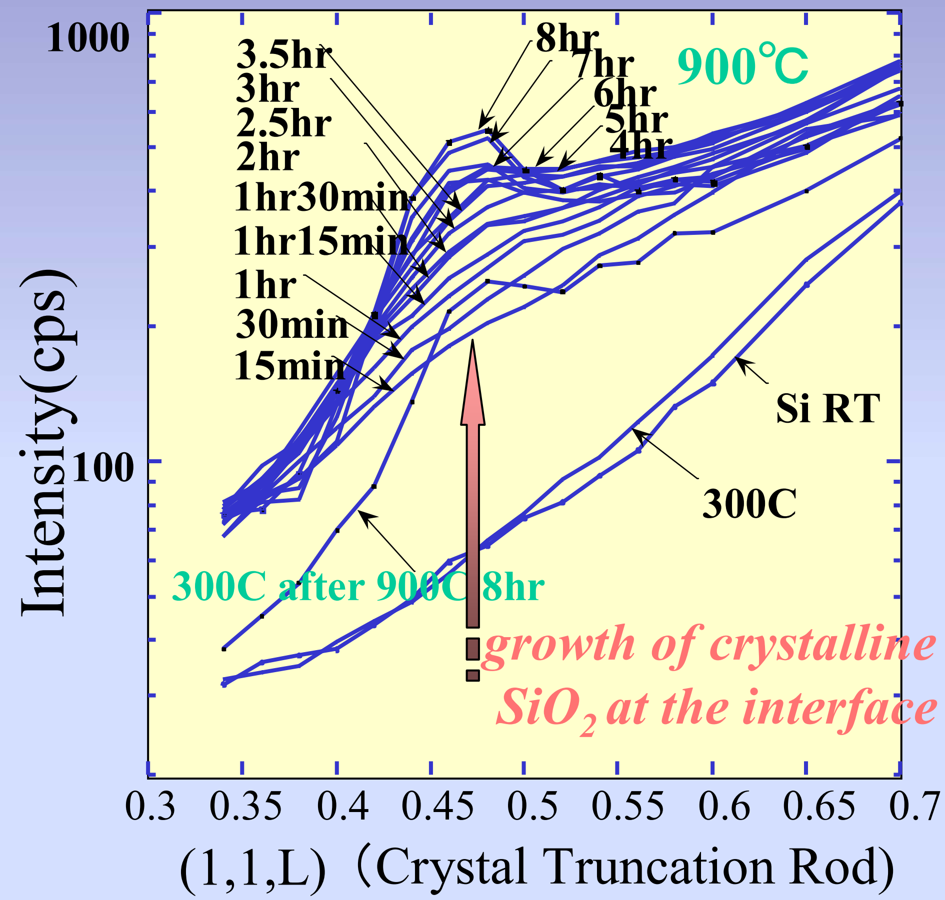

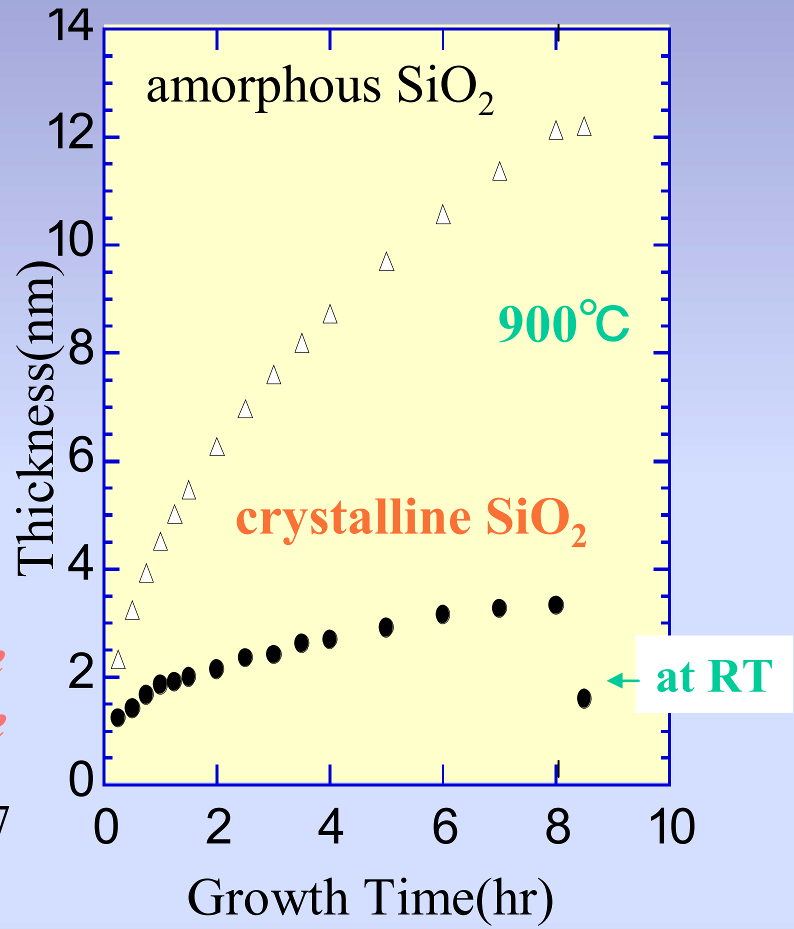

interface layer = oxidation front : ～1 nm at RT
fundamental phenomena on thermal oxidation

N.Awaji Appl. Phys. Lett., 74(1999)2669.

Analysis of Si-oxidation by XPS

SiO_2 (～0.6 nm) on Si(001)2x1 hν =130eV Si2p

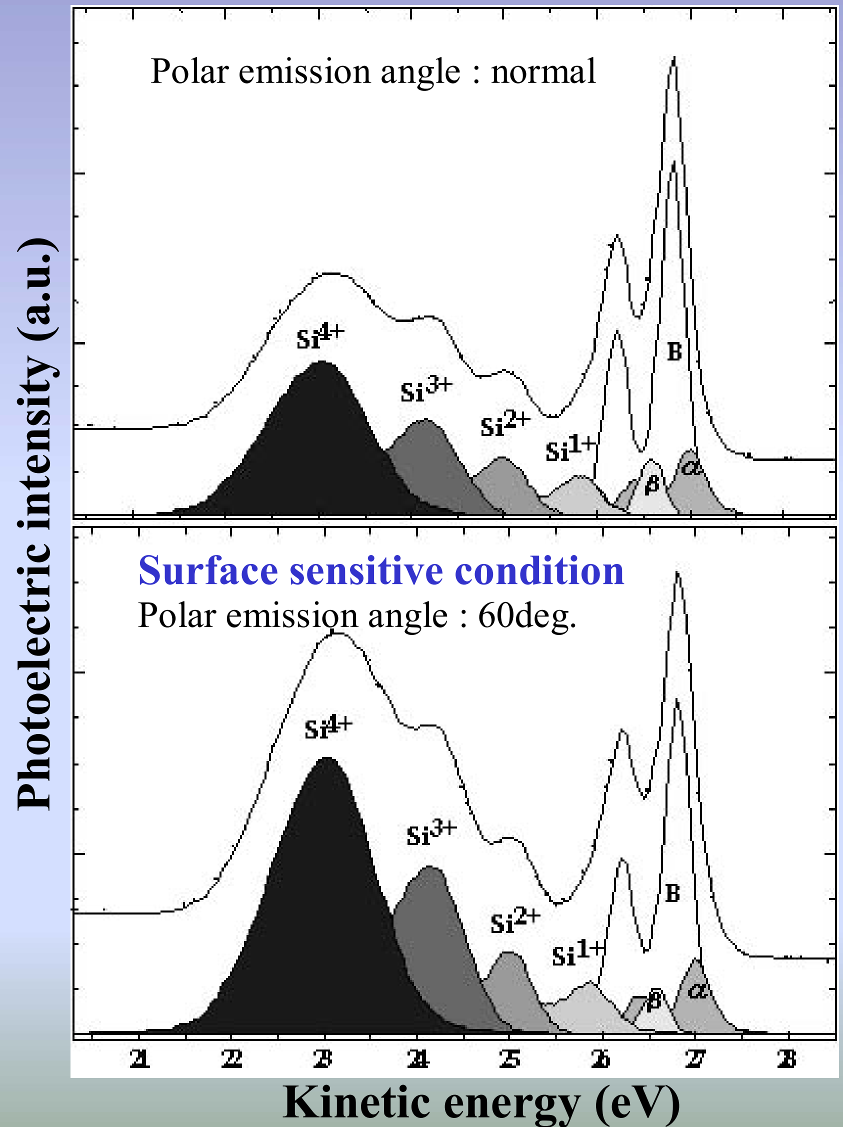

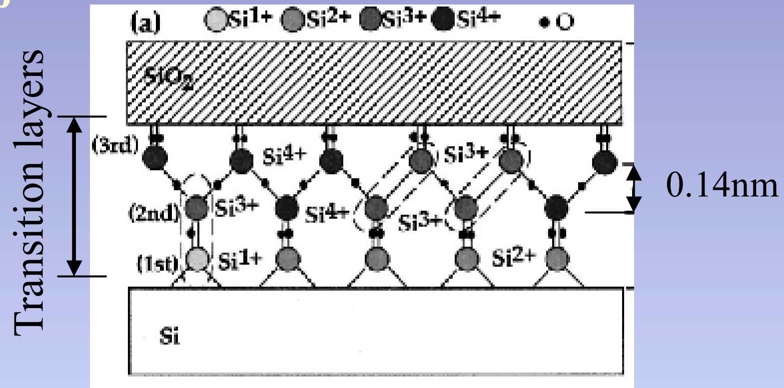

Transition layer model

3rd Si^{3+}/Si^{4+} ($Si^{3+} \ll Si^{4+}$)

2nd Si^{3+}/Si^{4+} ($Si^{3+} < Si^{4+}$)

1st Si^{1+}/Si^{2+} ($Si^{1+} < Si^{2+}$)

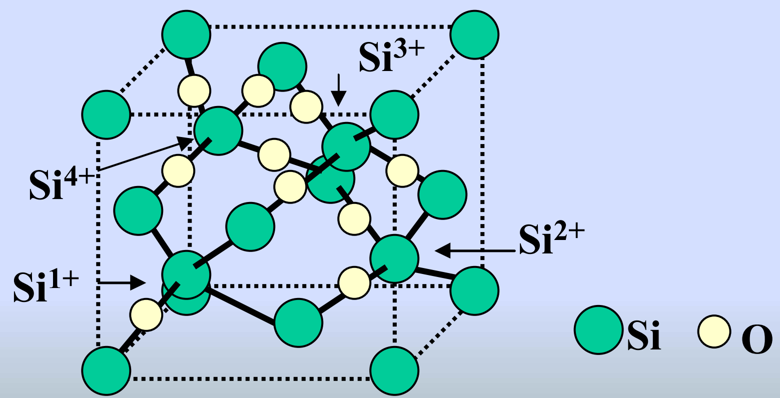

J.H. Oh et al., Phys. Rev. B63, 205310 (2001)

Hard Disk Drive

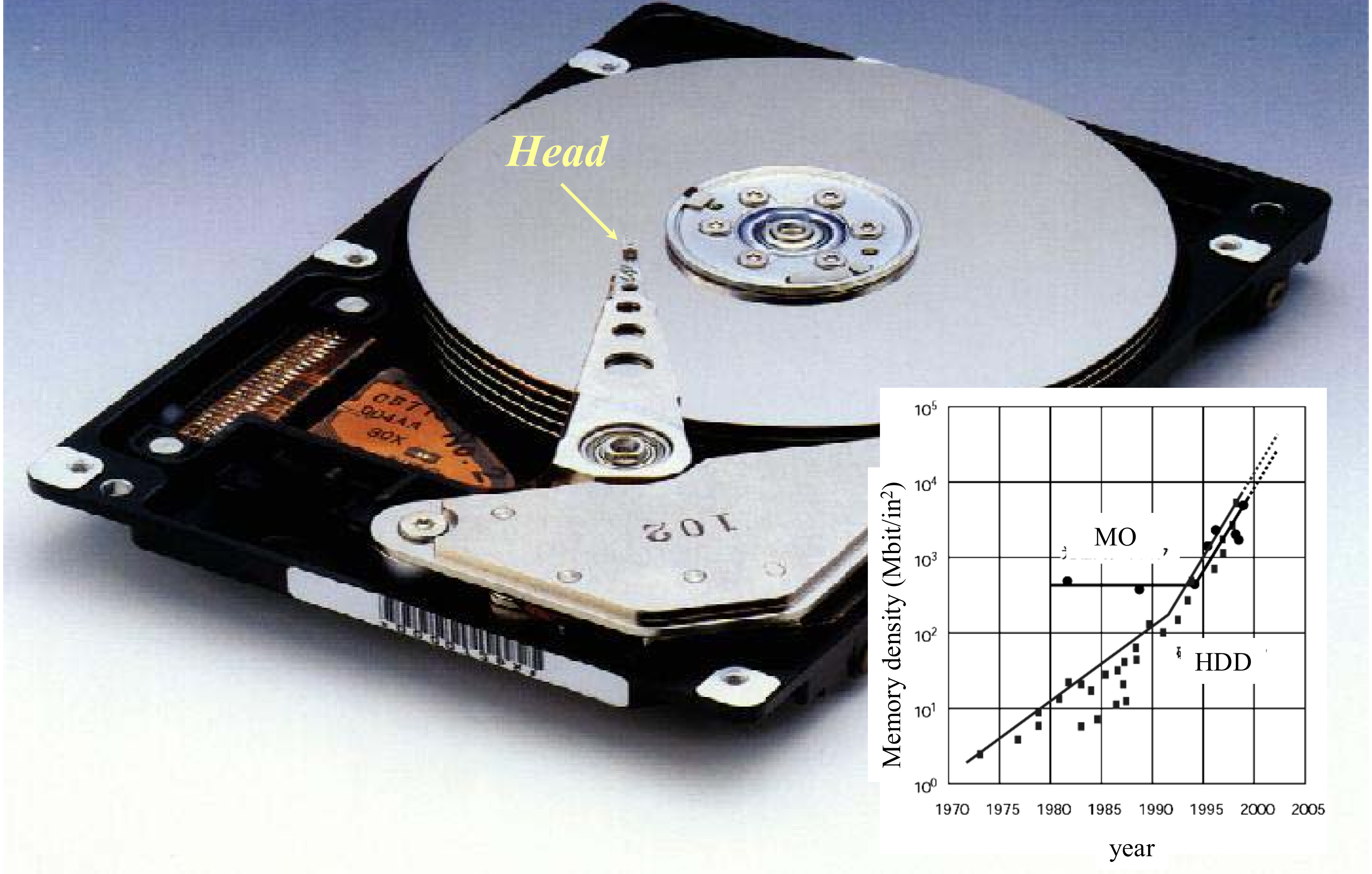

X-ray reflectivity analysis of multi-layers

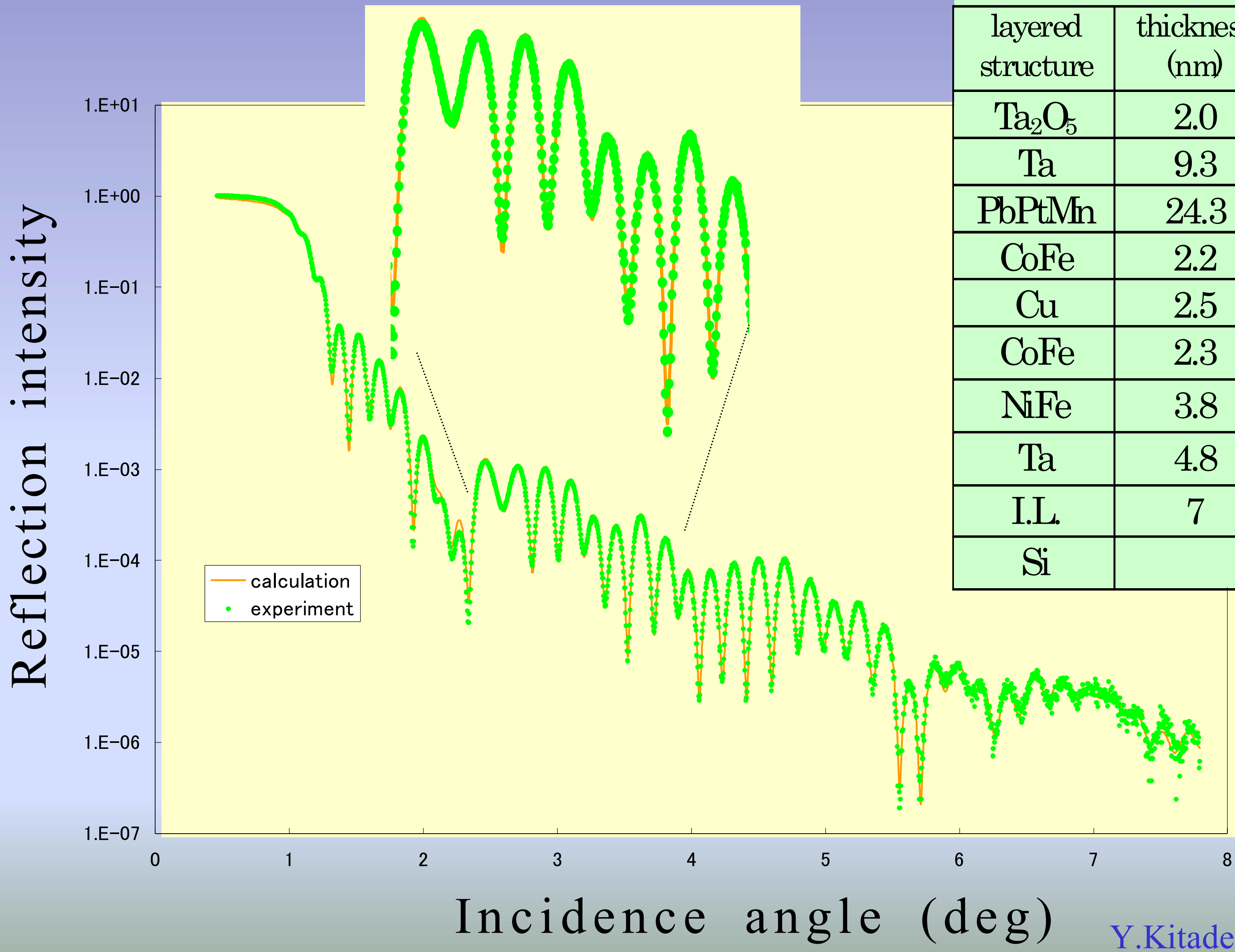

layered structure	thickness (nm)	rouphness (nm)
Ta_2O_5	2.0	0.6
Ta	9.3	0.5
PbPtMn	24.3	0.5
CoFe	2.2	0.4
Cu	2.5	0.5
CoFe	2.3	0.4
NiFe	3.8	0.3
Ta	4.8	0.4
I.L.	7	0.2
Si		0 3

Y.Kitade in Fujitsu Labs.

Wavelength dispersive X-ray fluorescence

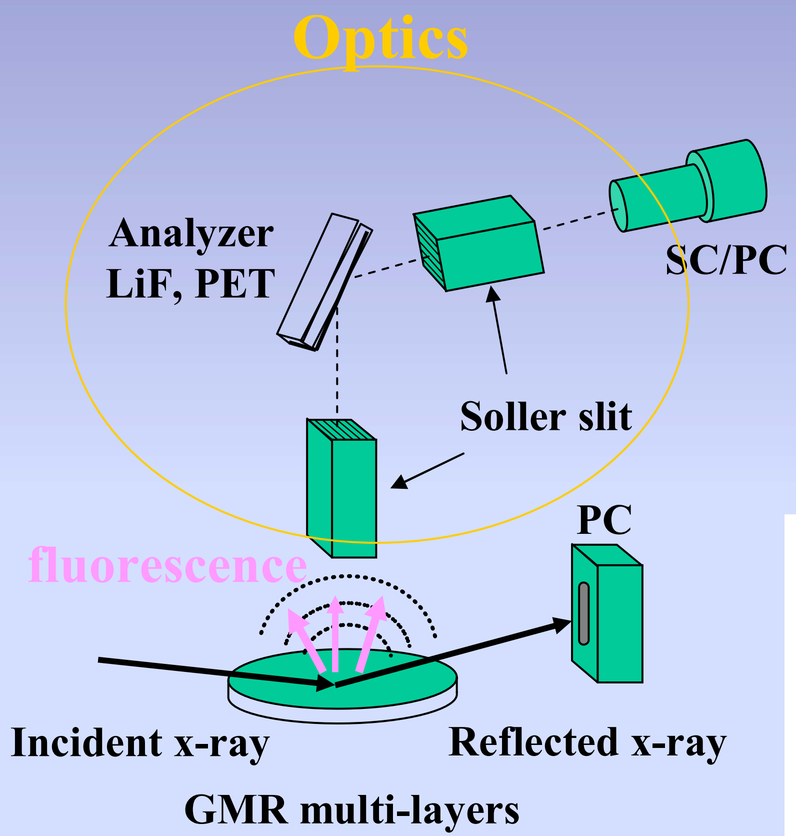

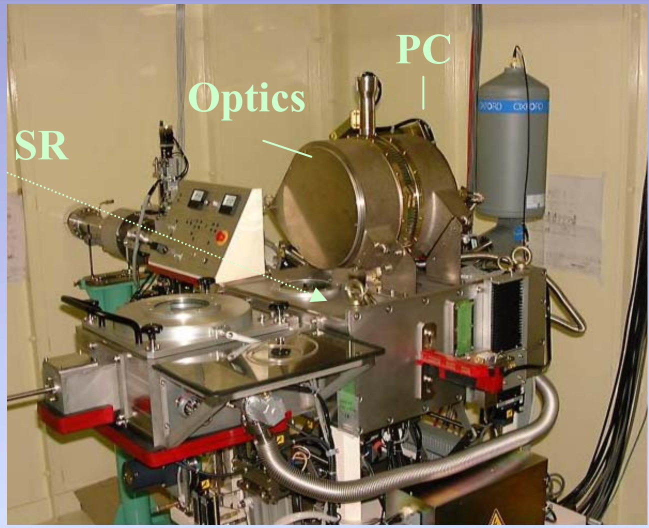

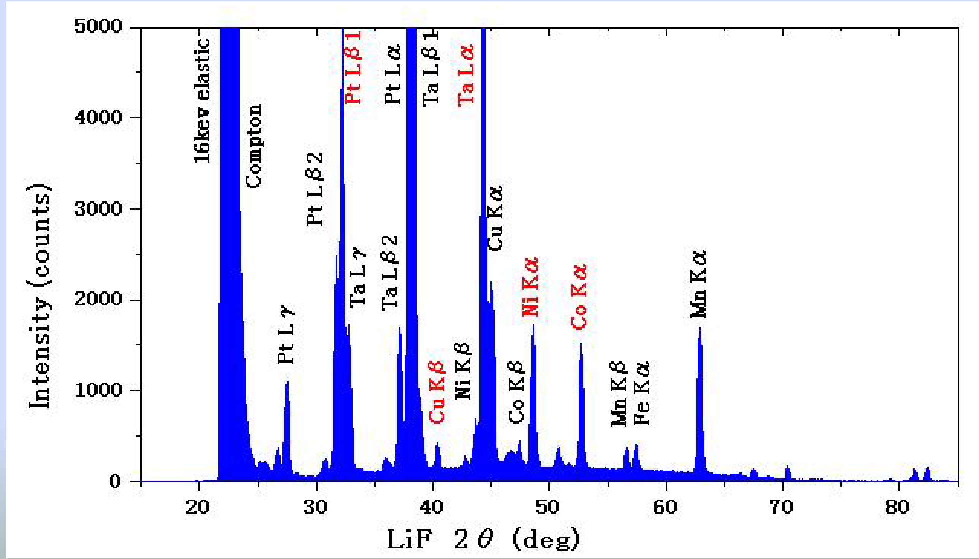

Fluorescence spectra from spin-valve multi-layers with grazing incidence

Grazing Incidence X-ray Fluorescence Technique

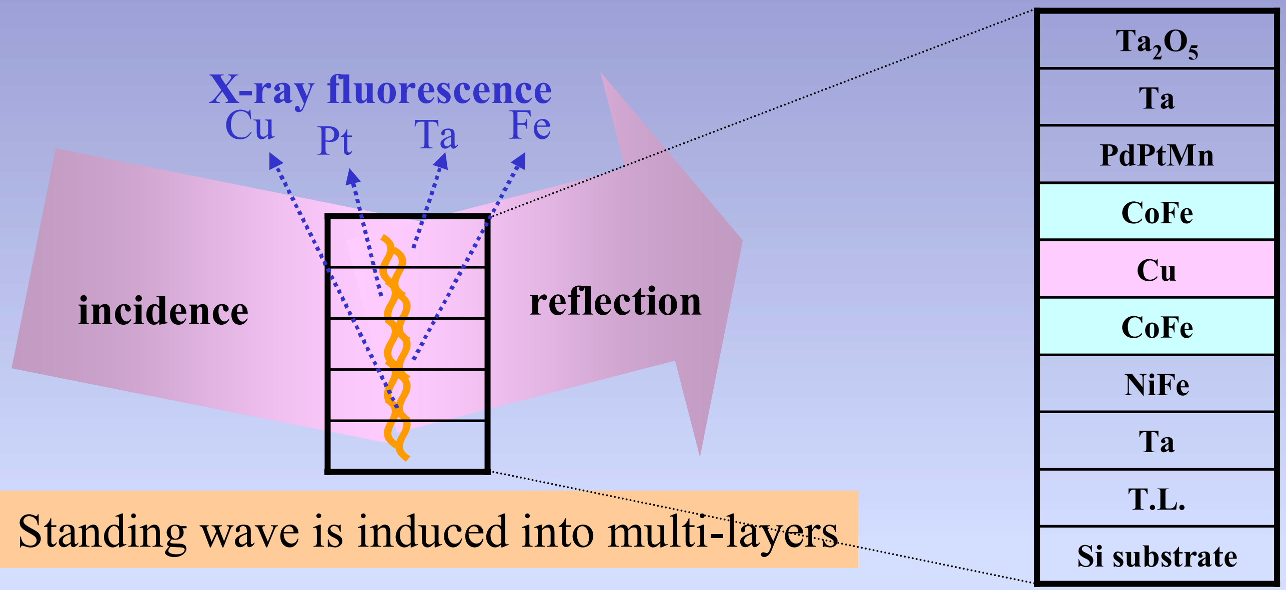

Standing wave is induced into multi-layers

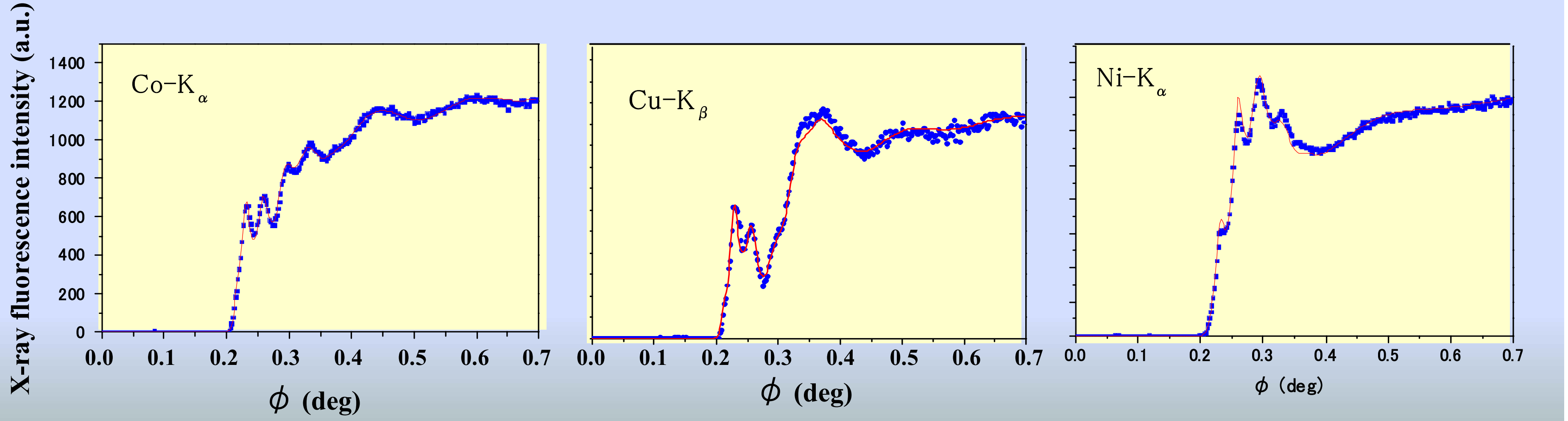

X-ray incident angle (deg)

Broadening of the interfaces in GMR multilayers

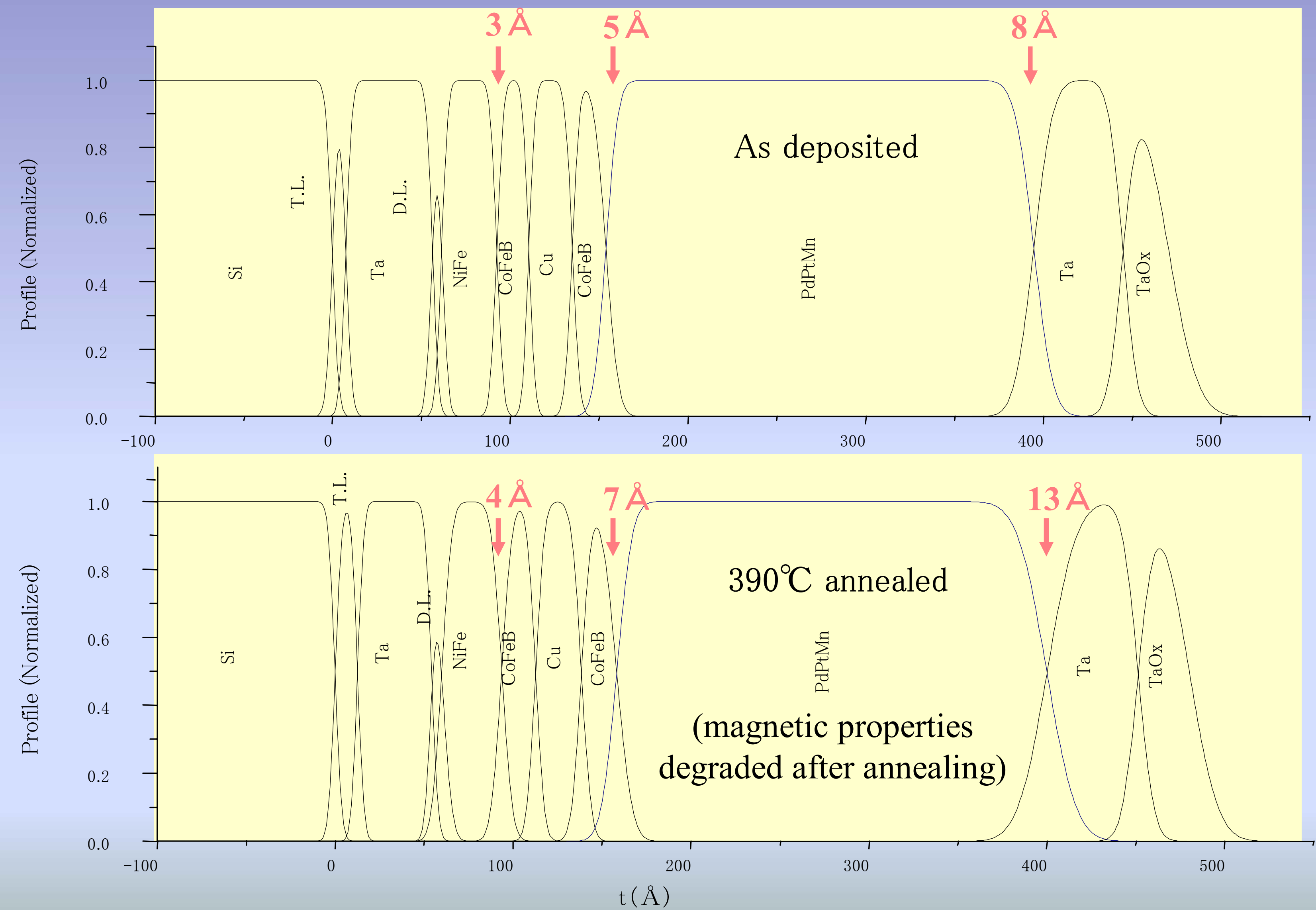

Depth profiles of elements analyzed from GIXF and reflectivity data

N.Awaji Fujitsu scientific & technical journal 38 (2002) 82.

record along a circle and in-plane magnetization

texture ⟹ magnetization along a circle

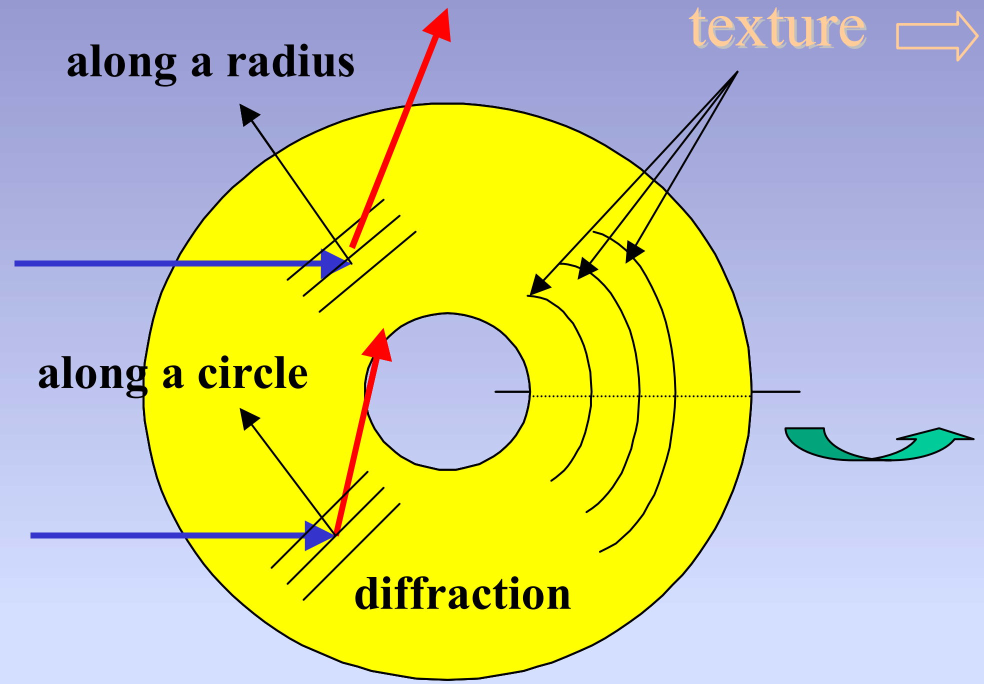

hard disk

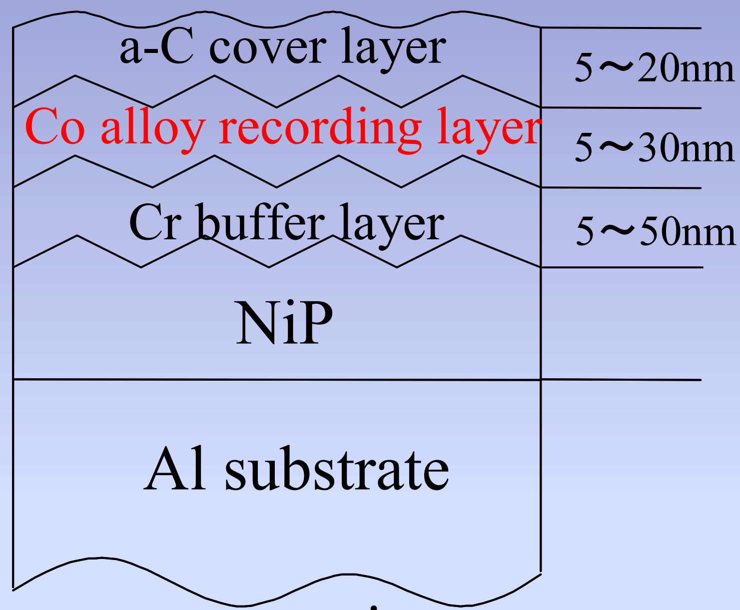

cross section

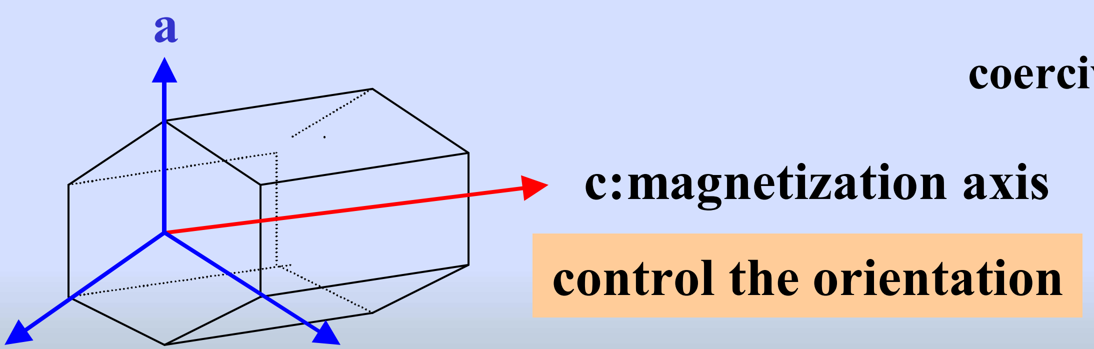

Co alloy : hcp crystal

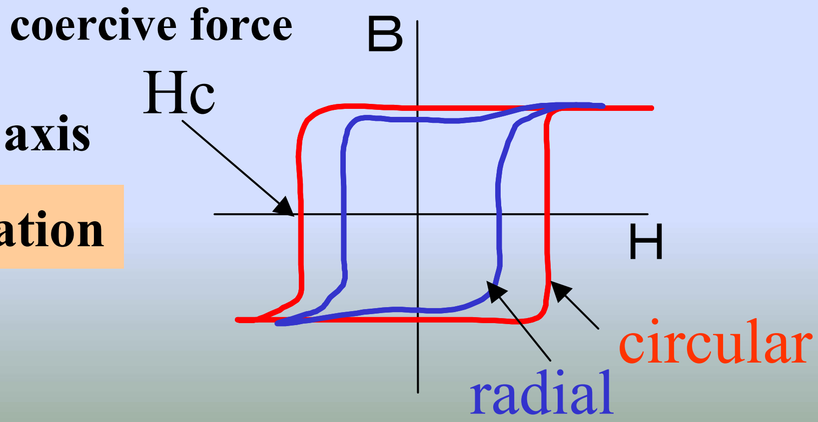

Grazing incidence x-ray diffraction profiles

Textured-Al/NiP/Cr/Co-alloy(**20nm**)/a-C

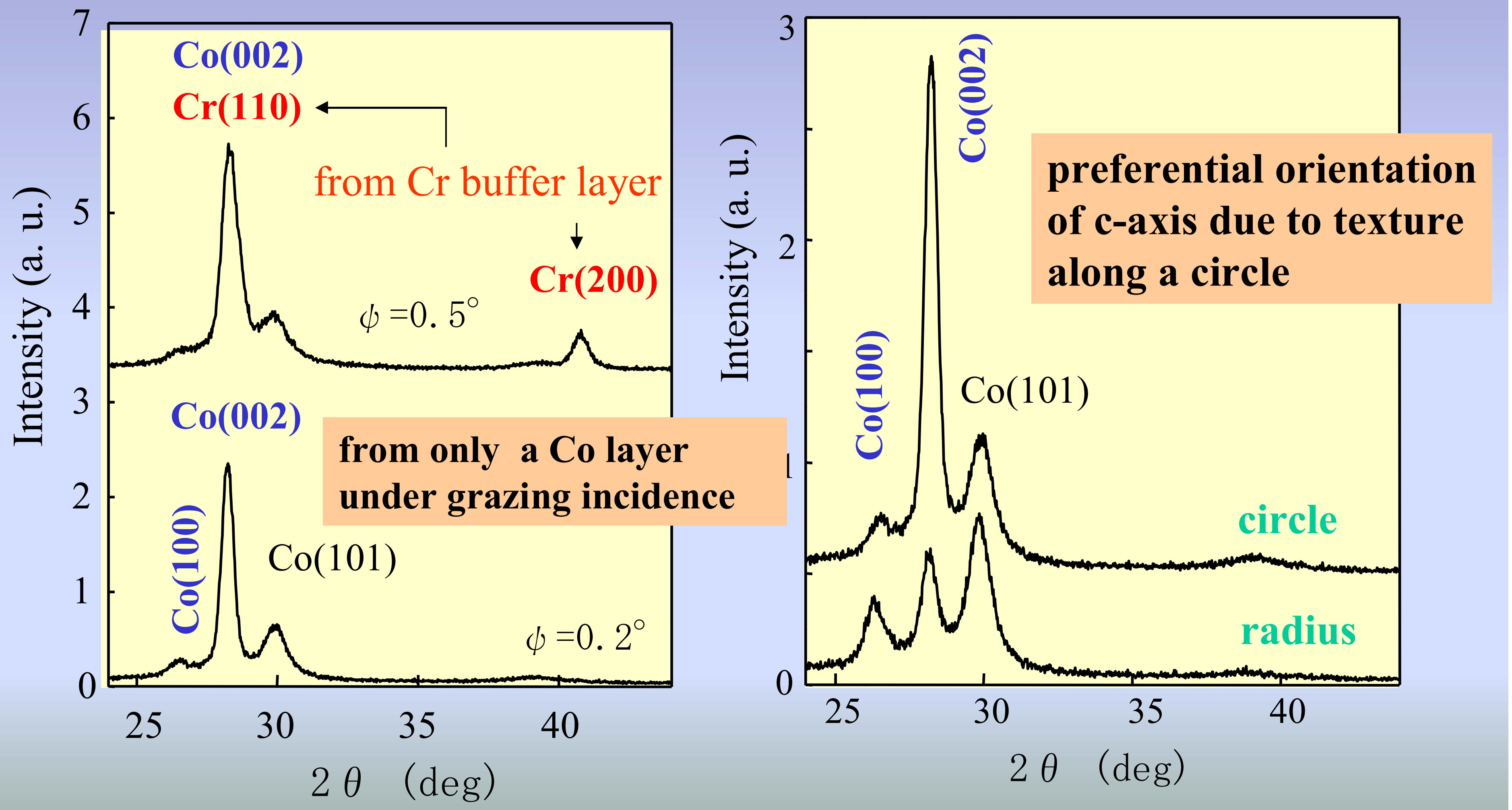

Preferential c-axis orientation dependence of coercive magnetic force

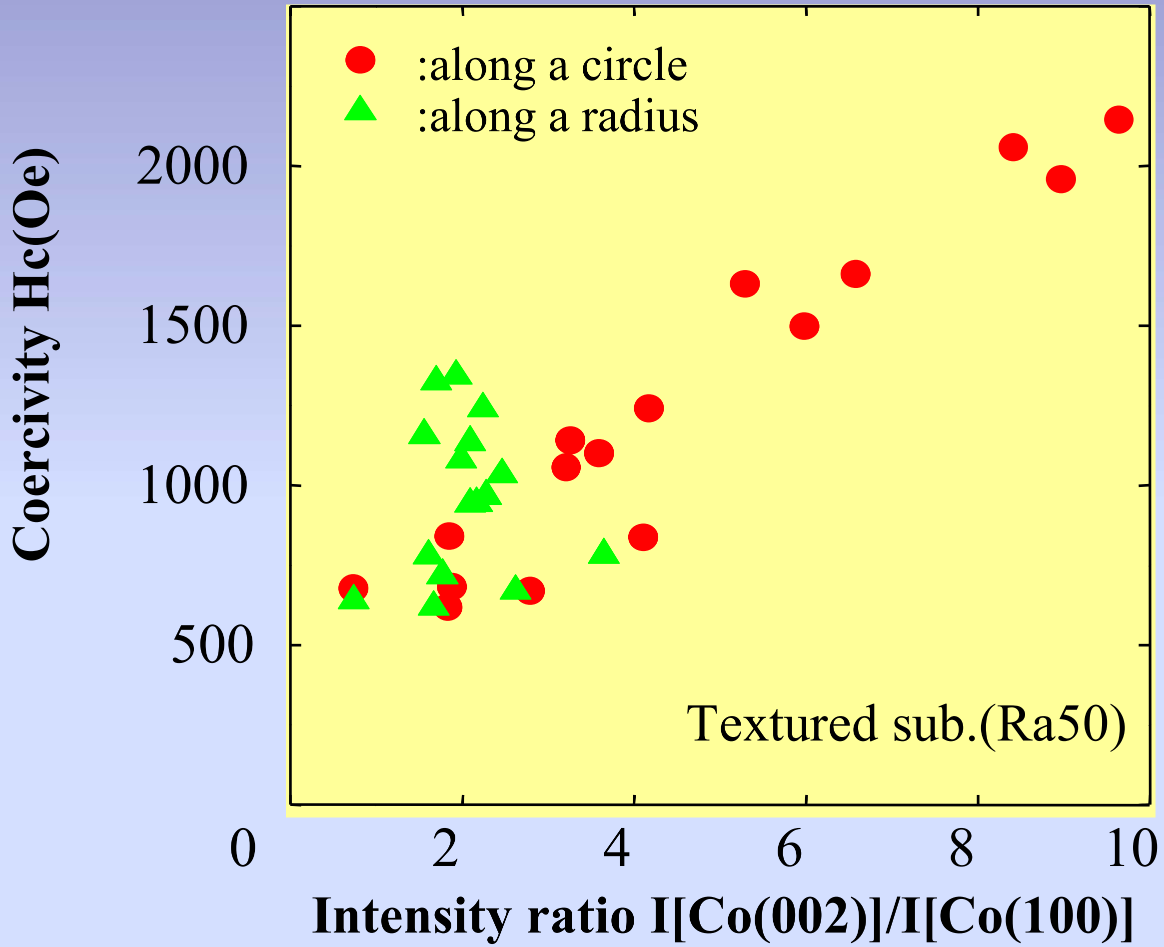

Increase in coercive force due to preferential c-axis orientation along a circle

T.Hirose IEEE Trans. Mag. 33. (1997) 2971.

Blue laser for DVD optical storage devices

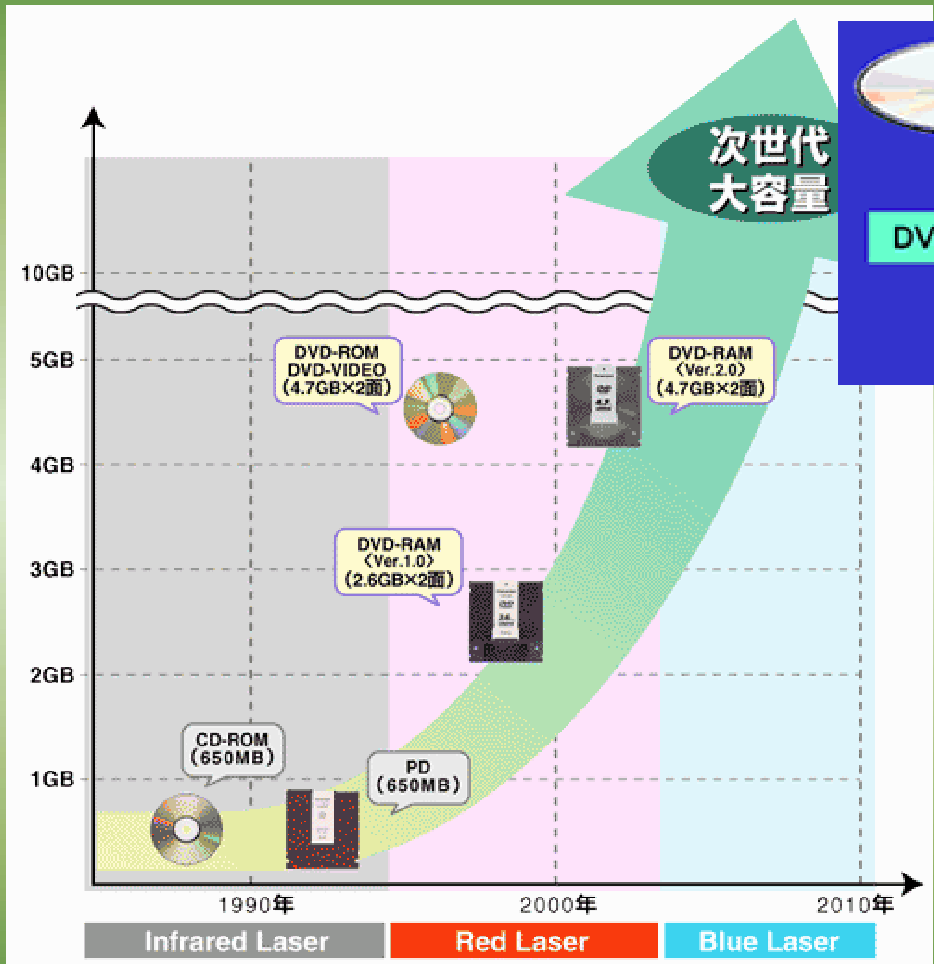

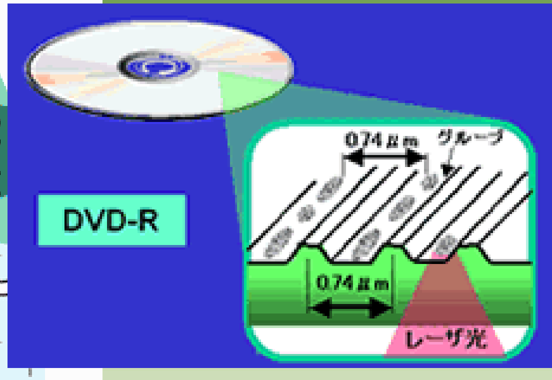

Red: GaAlAs

Blue: $Ga_{1-x}In_xN$

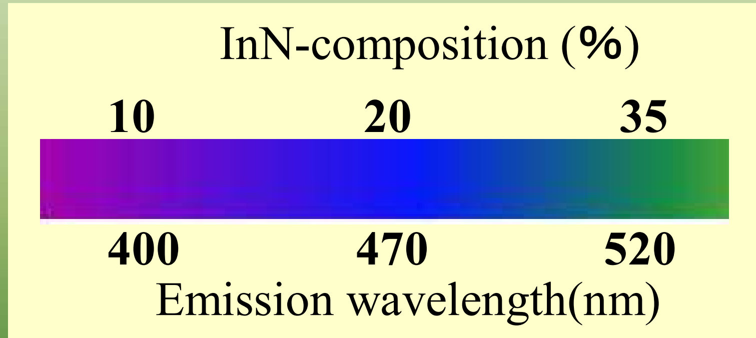

How is local structure in GaInN with low In composition less than 20% which is the critical composition for the phase separation?

InN composition dependence of GaInN XAFS

XAFS spectra around In K edge measured in the fluorescence mode

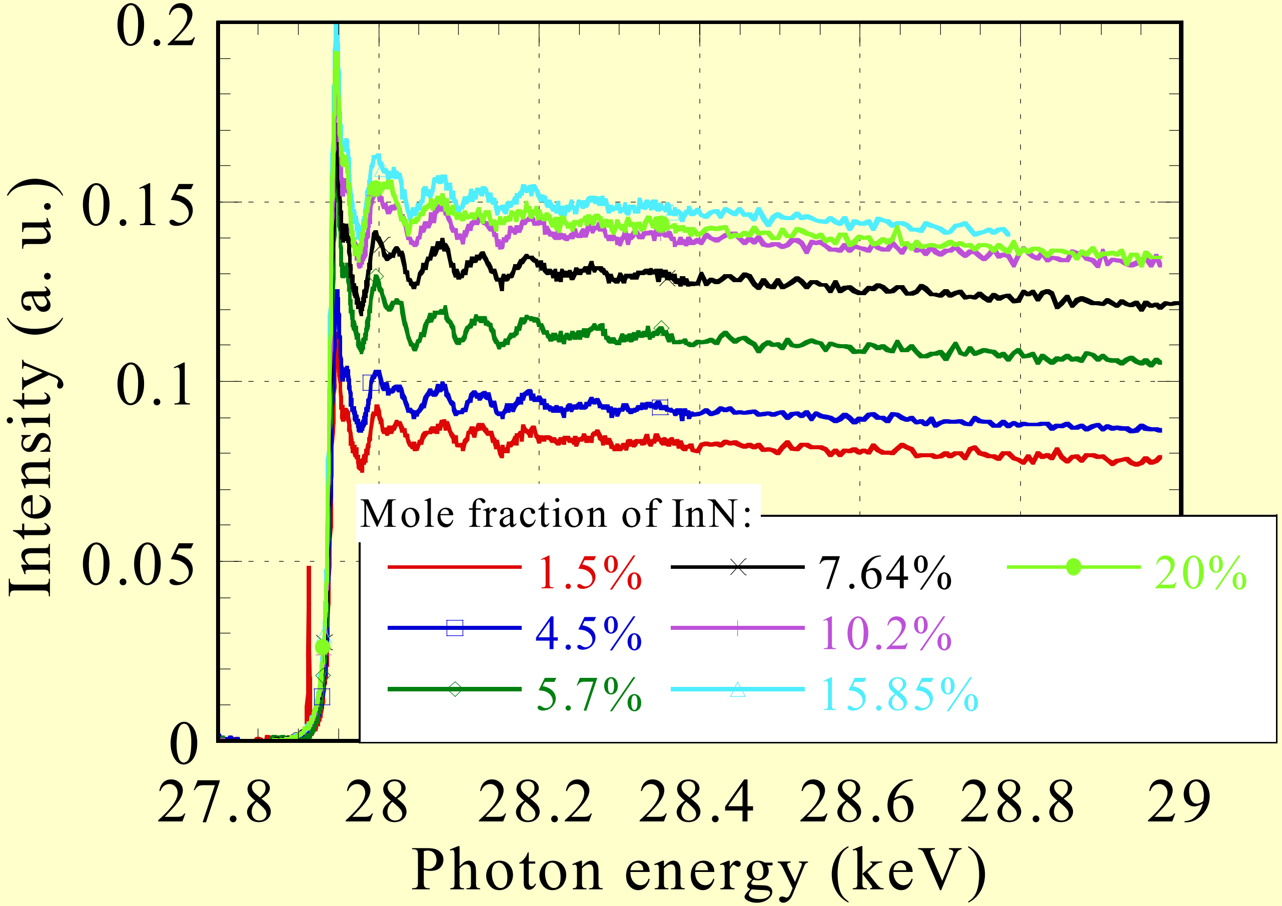

InN composition dependence of radial distribution functions

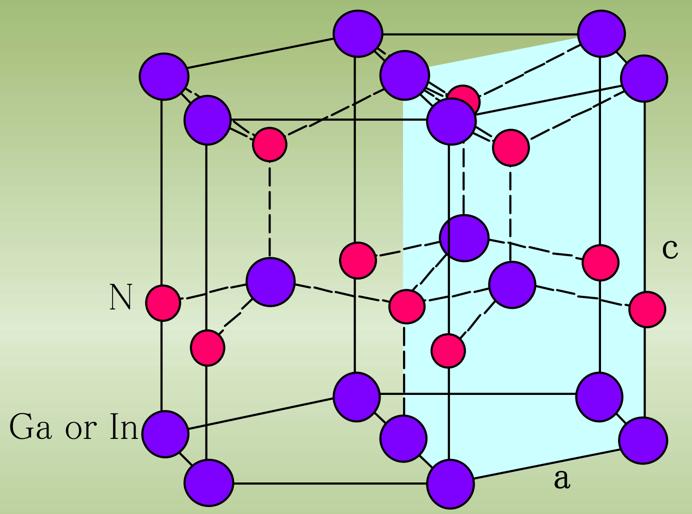

wurtzite crystal structure
(a=3.189Å, c=5.185Å for GaN)

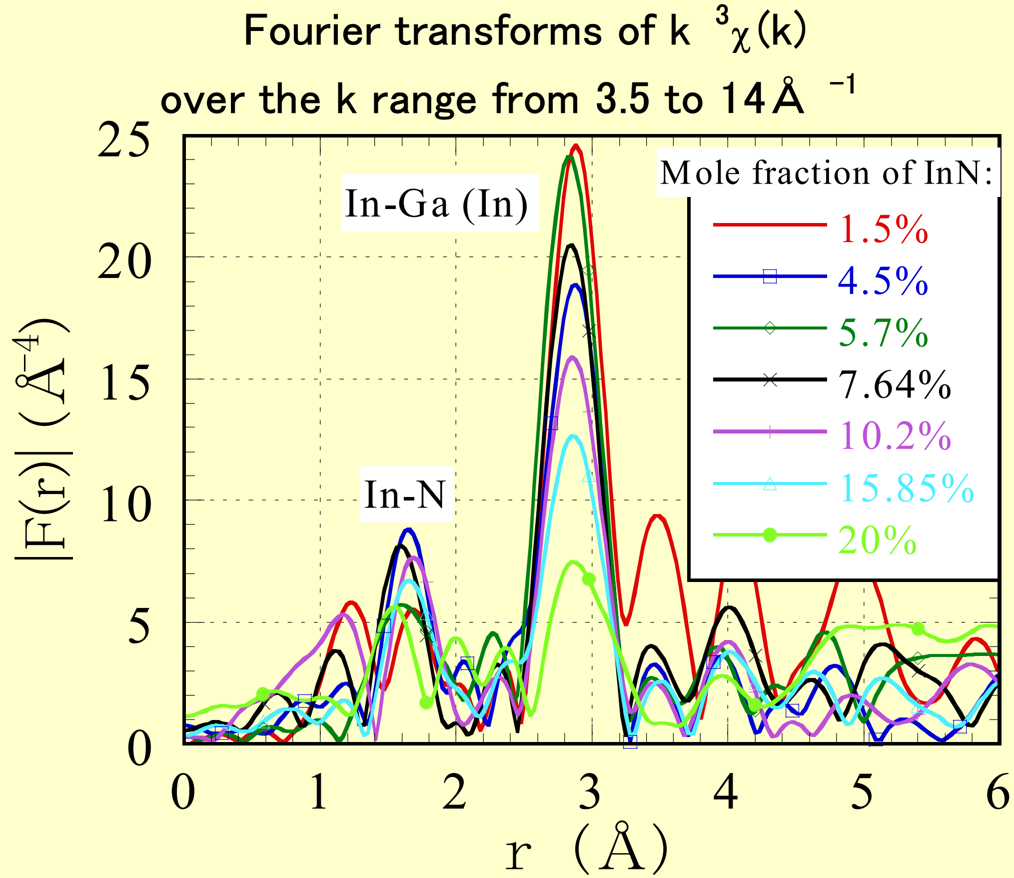

Monotonic decrease in the second peaks from In-Ga(In)

InN composition dependence of the local structure

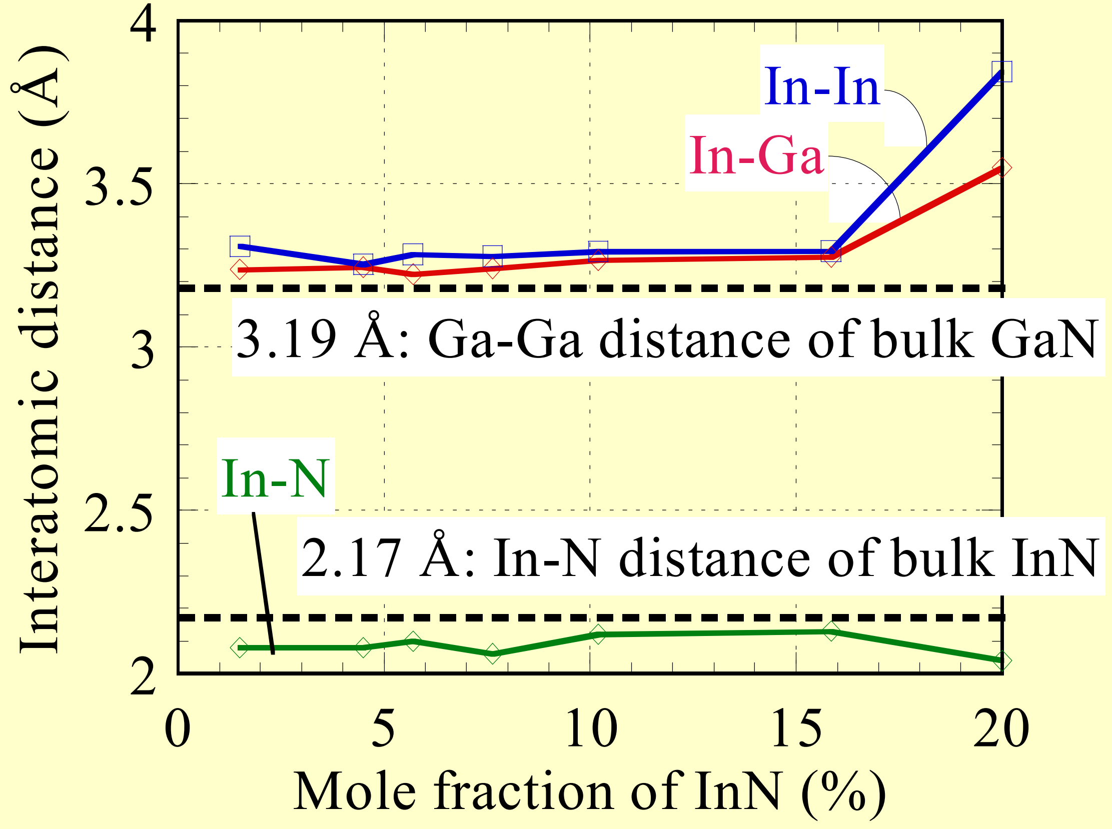

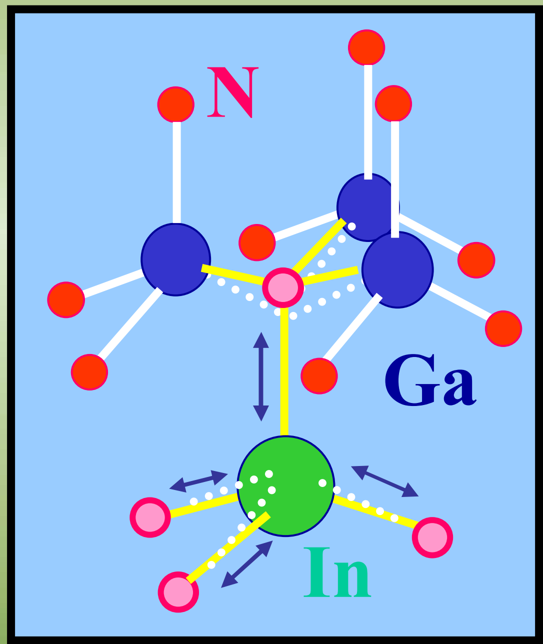

Change of bond angles

InN composition dependence of atomic distances

Deviation from random distribution of Ga and In atoms in GaInN mixed crystal

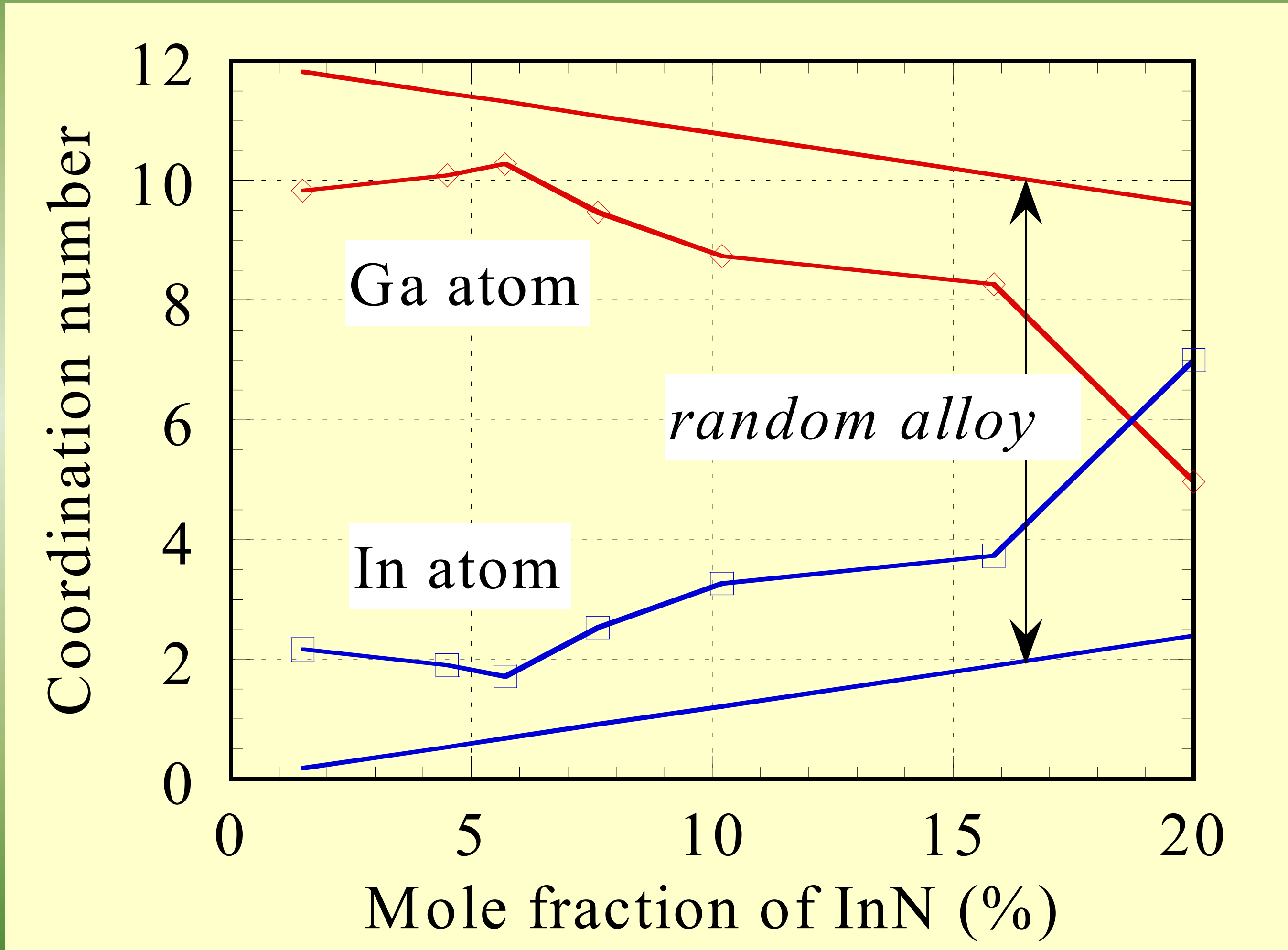

In composition dependence of the 2nd neighbor coordination numbers

T. Miyajima phys. Stat. Sol. (b) 228, 45 (2001).

Phase transition storage materials for DVD

ーAccurate structure analysis with a Debye-Scherrer cameraー

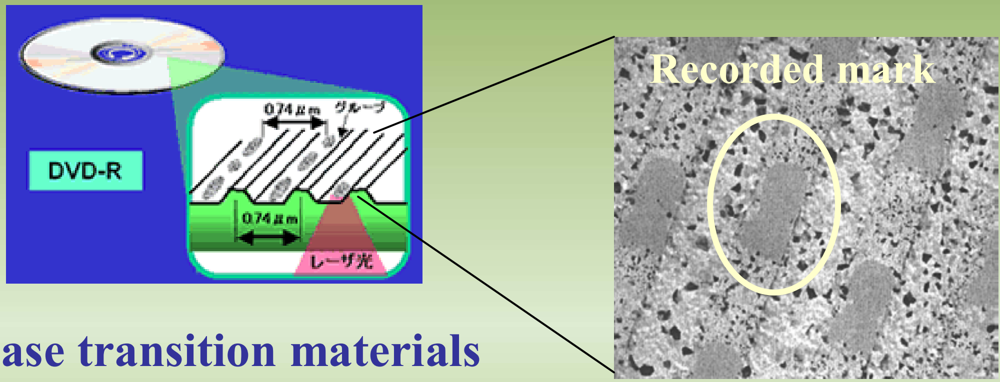

Phase transition materials

- AuGeSnTe
- GeSbTe
- AgInSbTe

Debye-Scherrer camera

Record&elimination by laser exposure

- High power→amorphous formation by quenching
- Low power→crystallization by annealing

What materials are excellent in high speed record/elimination and reliability

X-ray power diffraction with SR

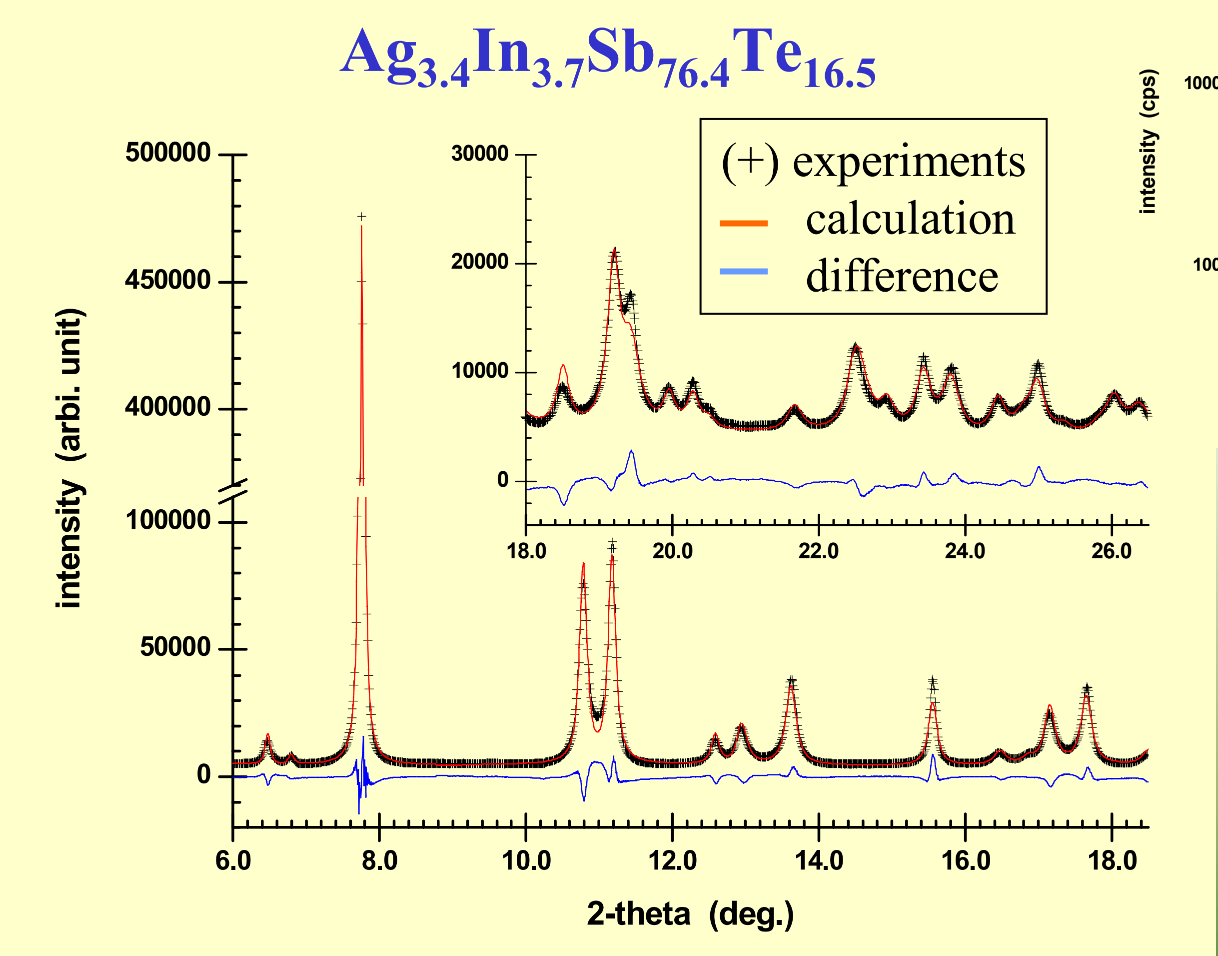

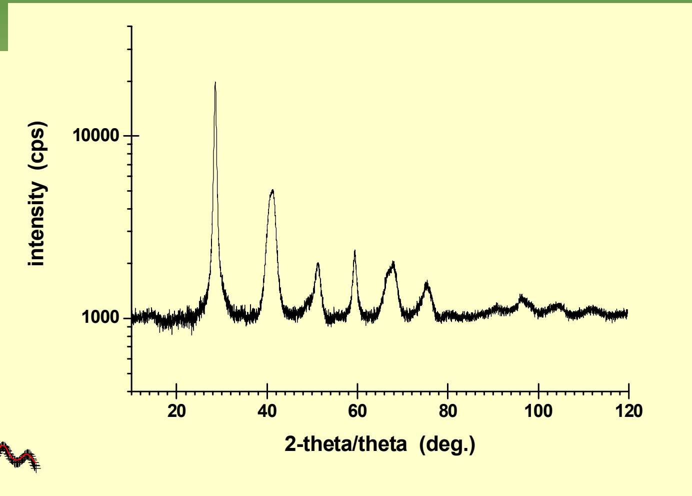

With a laboratory source

Excellent resolution

X-ray powder diffraction with SR source

Fine crystalline structure of AgInSbTe

$Ag_{3.4}In_{3.7}Sb_{76.4}Te_{16.5}$

At low temperature

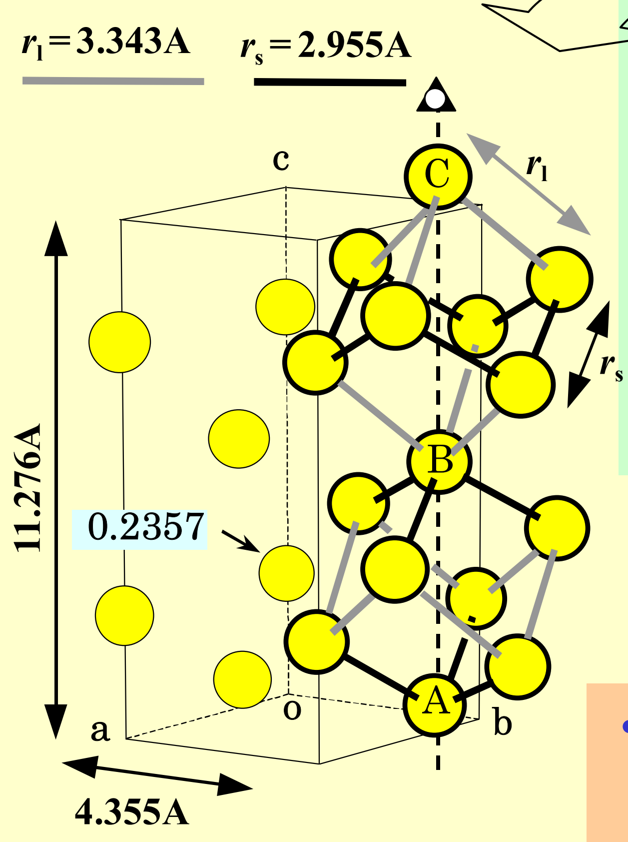

A7, $R\bar{3}m$

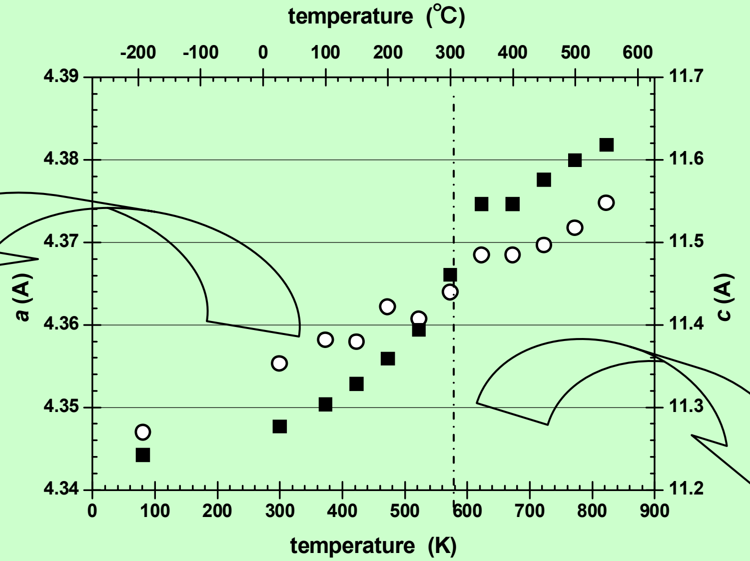

Temperature dependence of lattice parameteres

At high temperature

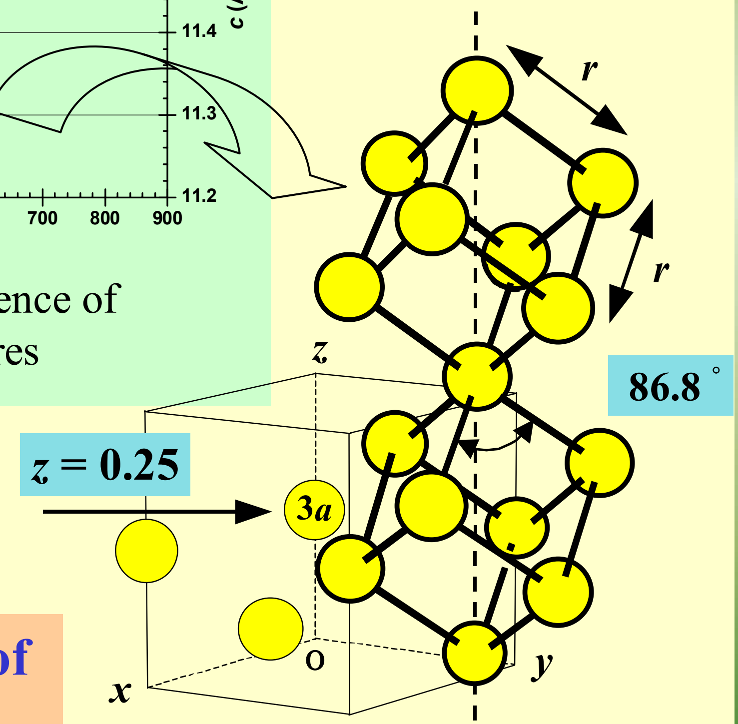

R32/R3m

- **Random occupancy of Ag, In, Sb, Te**
- **Simple cubic units**

T. Matsunaga Phys. Rev. B64 (2001)184116.

Common properties on three materials

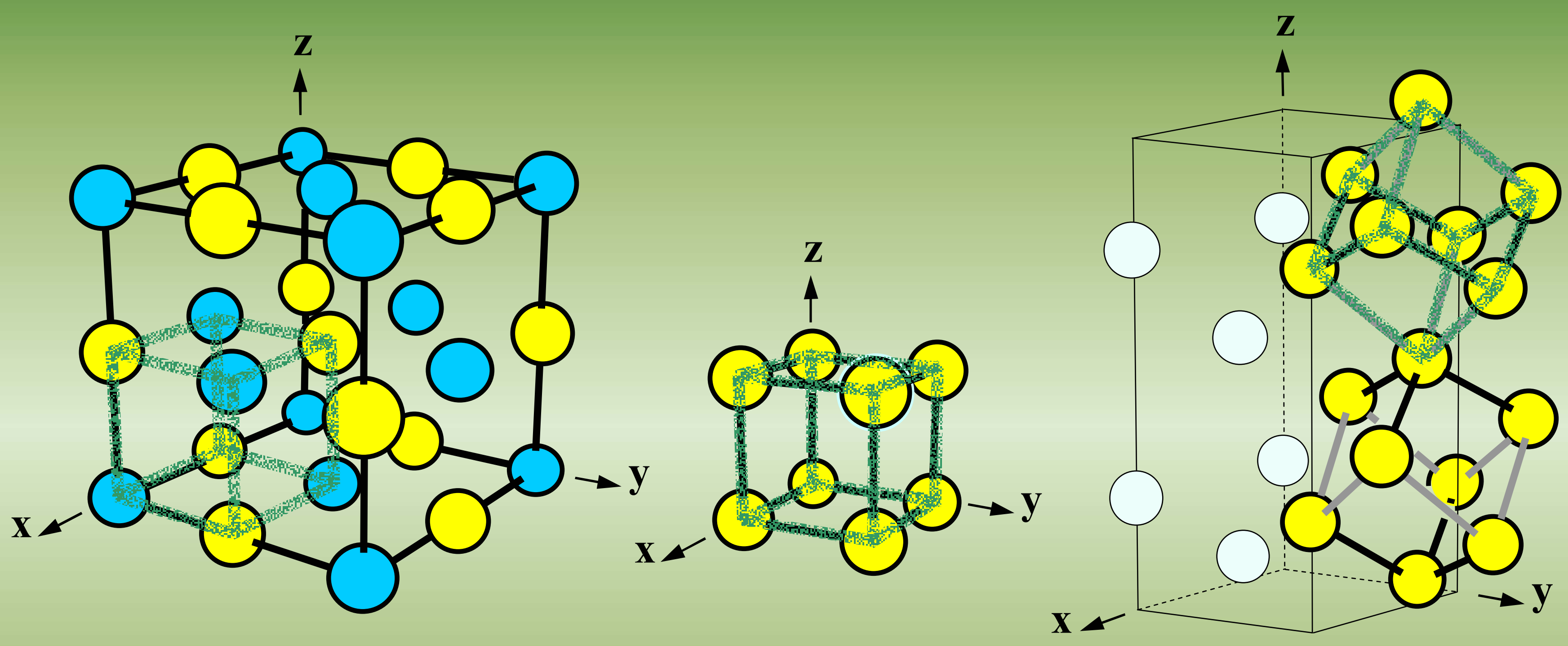

GeTe-Sb_2Te_3 $Au_{25}Ge_4Sn_{11}Te_{60}$ $Ag_{3.4}In_{3.7}Sb_{76.4}Te_{16.5}$

- Unique crystalline phase
- Poor package :simple cubic, allowance of many vacancies
- Random occupancy of component atoms at lattice sites

Development of laser diodes for optical communications

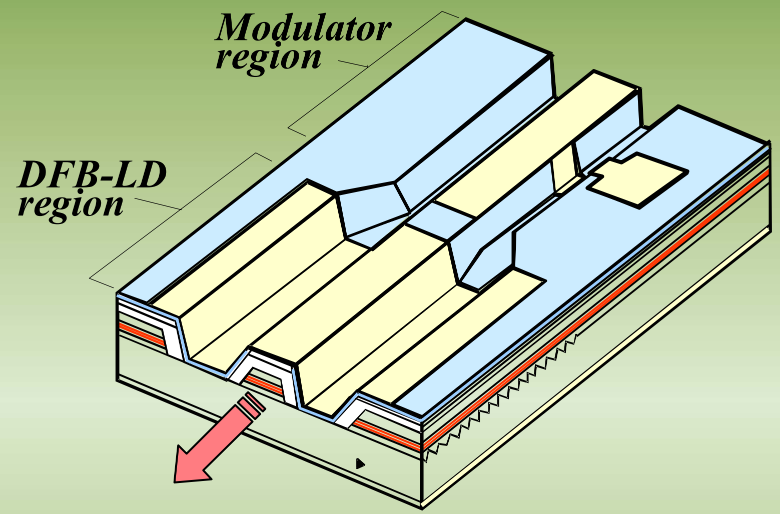

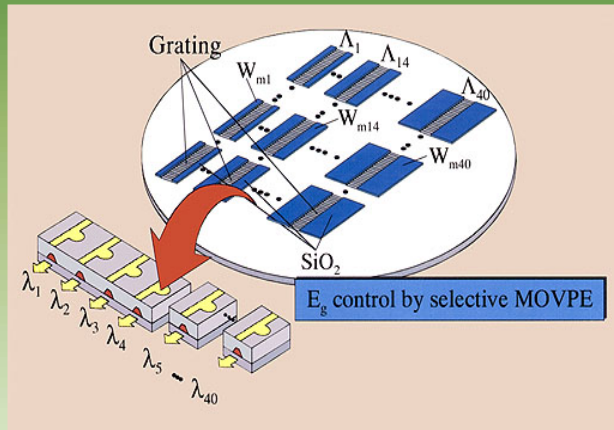

A package process for fabrication of lasers with various wavelength

DFB laser diode integrated with wave length modulator for WDM optical communications system

Control of wave length

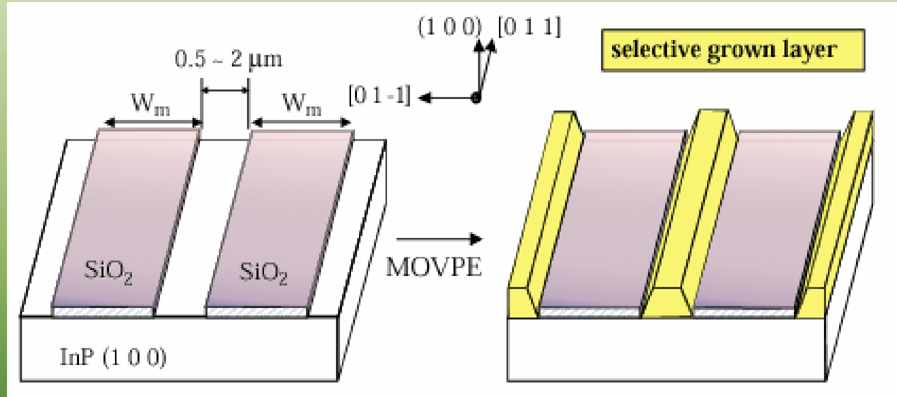

Narrow-strip selective metal-organic vapor phase epitaxy (MOVPE)

X-ray micro-beam

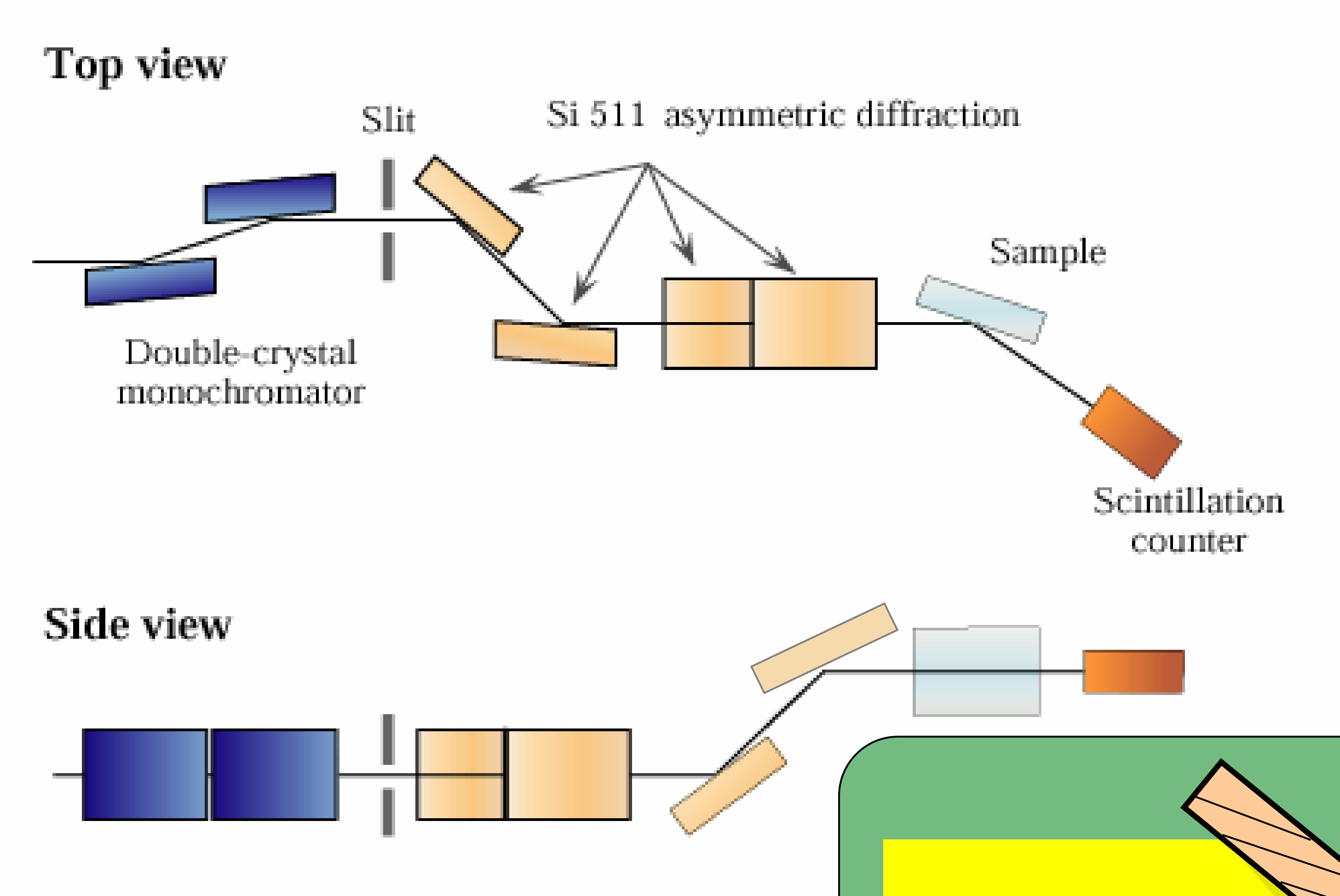

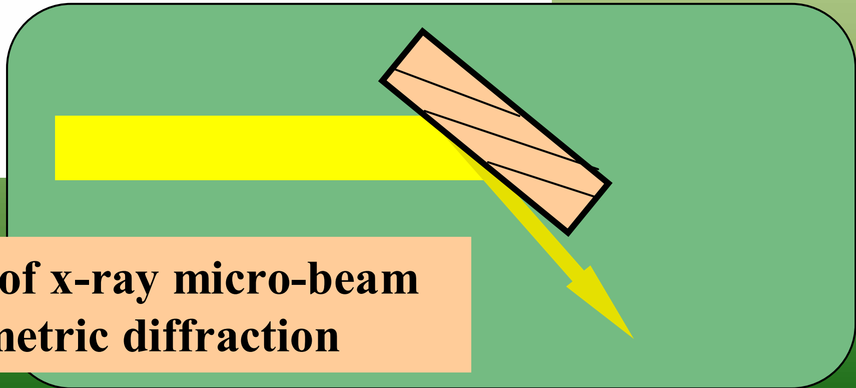

Formation of x-ray micro-beam with asymmetric diffraction

Determination of process condition

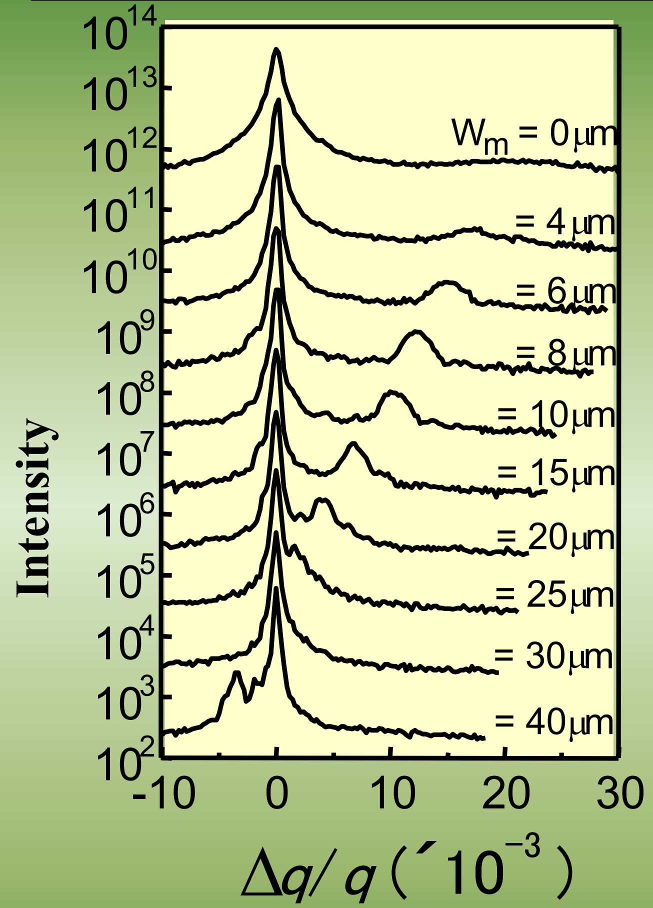

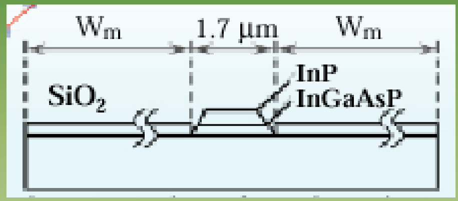

S.Kimura et al., APL 77(2000) 1286.

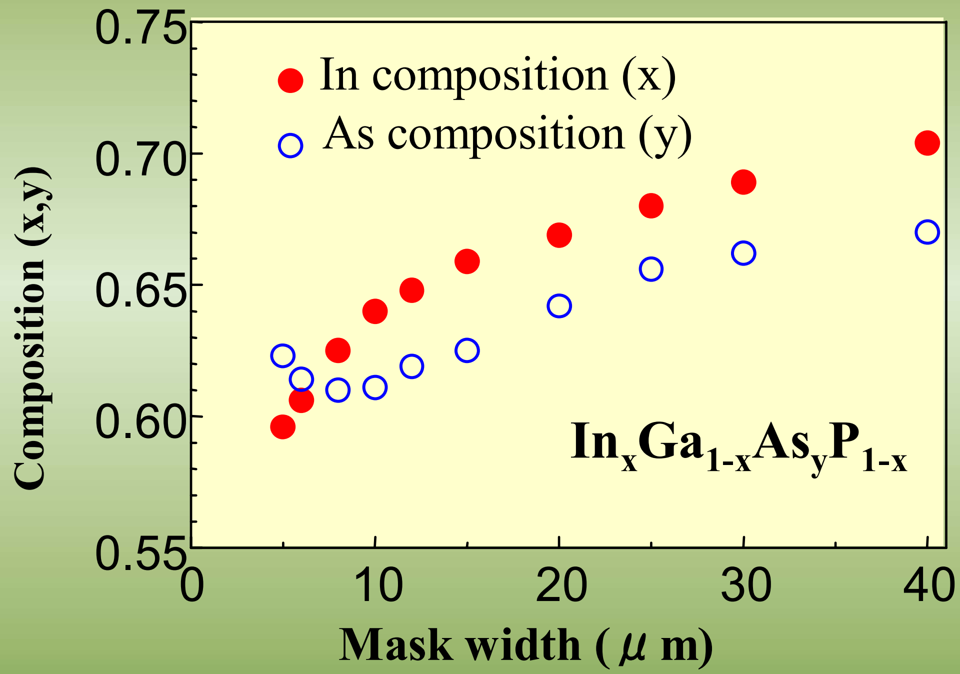

Mask width dependence of lattice parameter

Mask width dependence of composition (x,y)

40% up on emission efficiency of semiconductor laser

X-ray fluorescence analysis

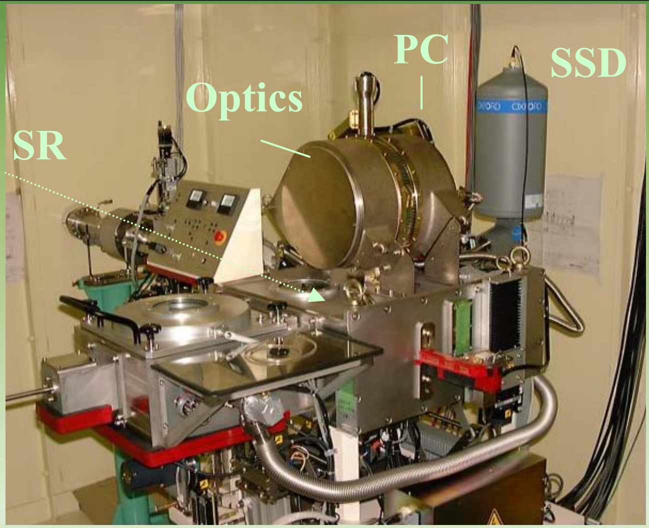

Energy dispersive (EDX)

- High sensitivity
- Low energy resolution

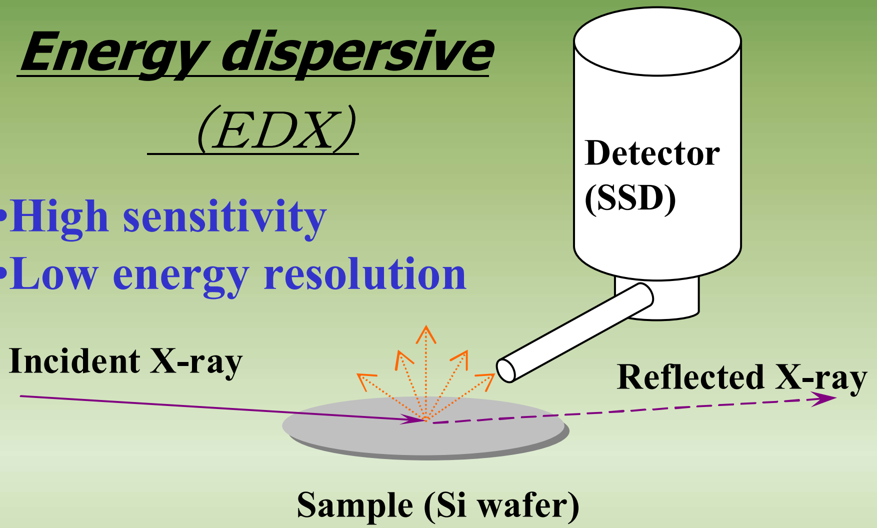

Wave dispersive (WDX)

- low sensitivity
- high energy resolution

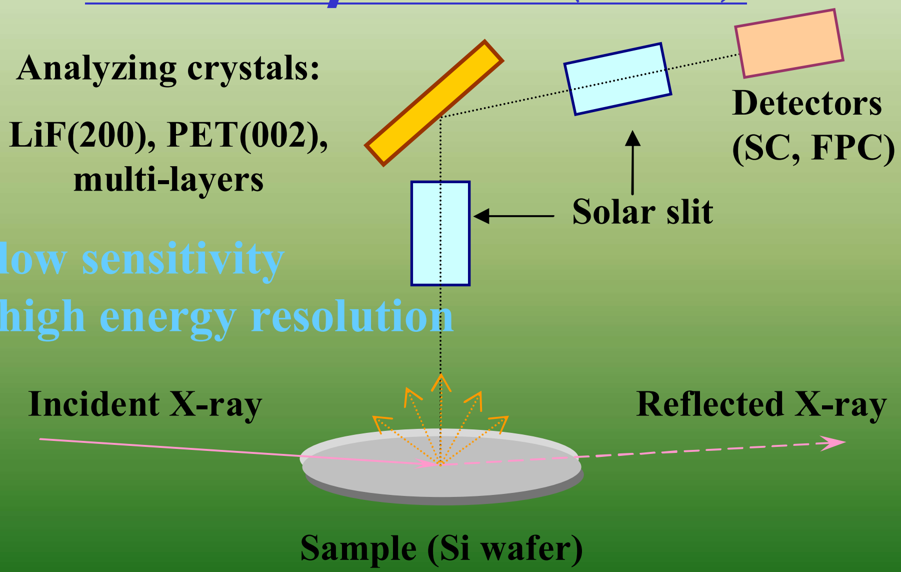

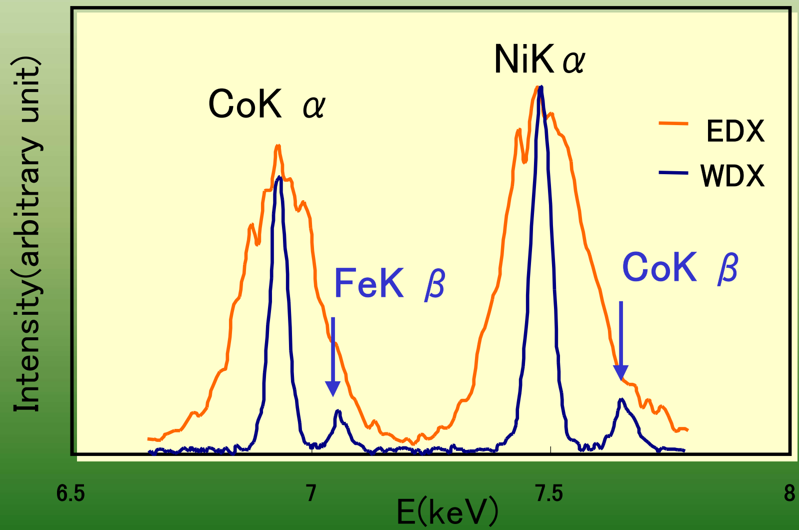

Ultra-low detection limit

M. Takemura in TOSHIBA

	2002	2005	2008	2011
size(nm)	130	100	70	50
production(bit)	1G	2G	-	16G
allowance ($\times 10^8$ atoms/cm^2)	≦4.4	≦2.5	≦2.1	≦1.8

ITRS road map

	Before concentration	After concentration
Ni	5×10^8	4×10^6
Cu	5×10^8	4×10^6
Al	2×10^{11}	8×10^8

atoms/cm^2

4×10^6 atoms/cm^2 = 4 atoms/100 μm^2

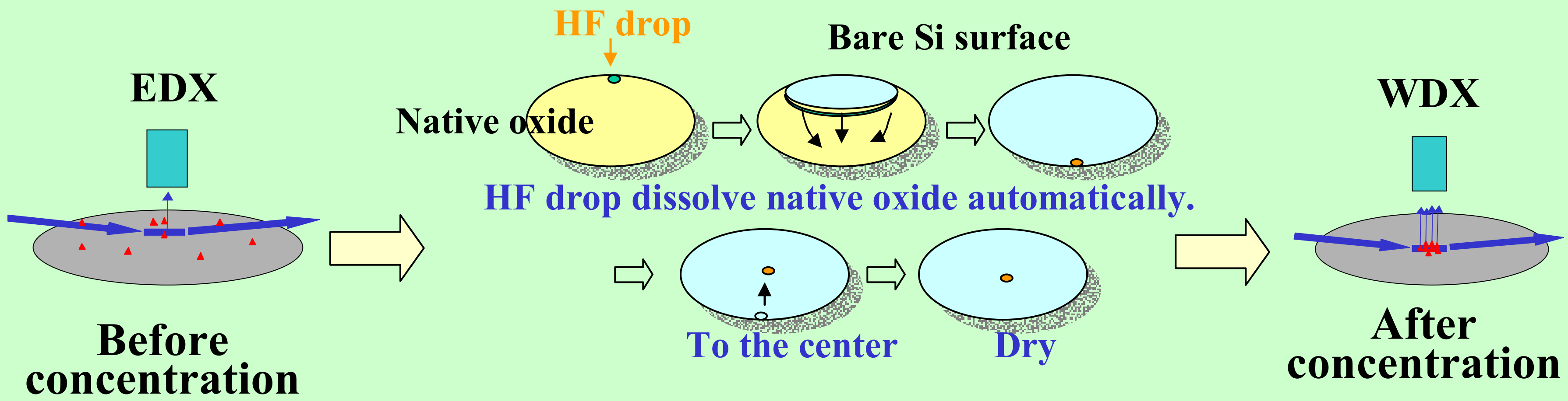

Concentration of contamination atoms

Direct observation of fibers in safety tire

SEM image

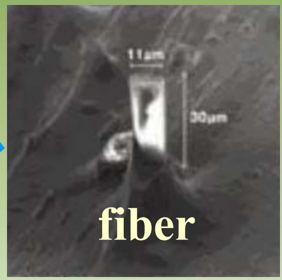

DUNLOP
SUMITOMO RUBBER INDUSTRIES, LTD.

Sharp edge image

Refractive contrast image

SR source

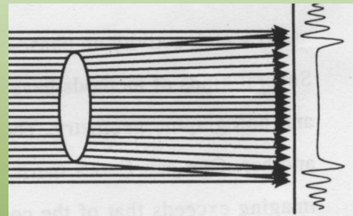

Difference of absorption

X-ray tube

press

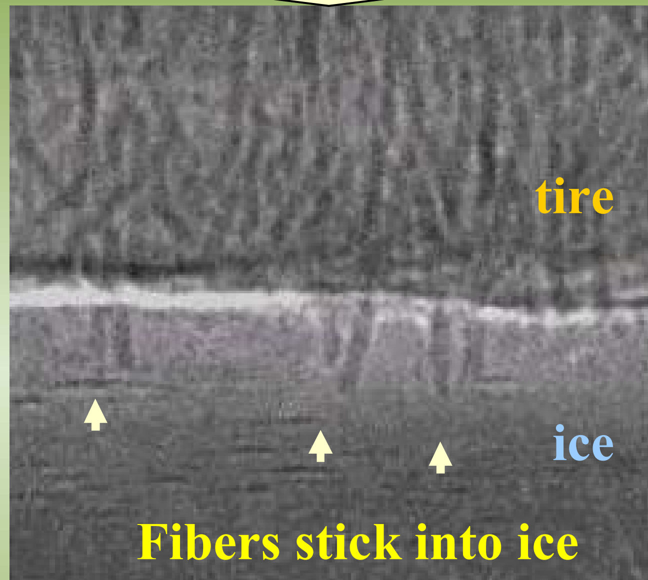

Direct observation of fibers sticking into ice

R&D on safety tire on ice

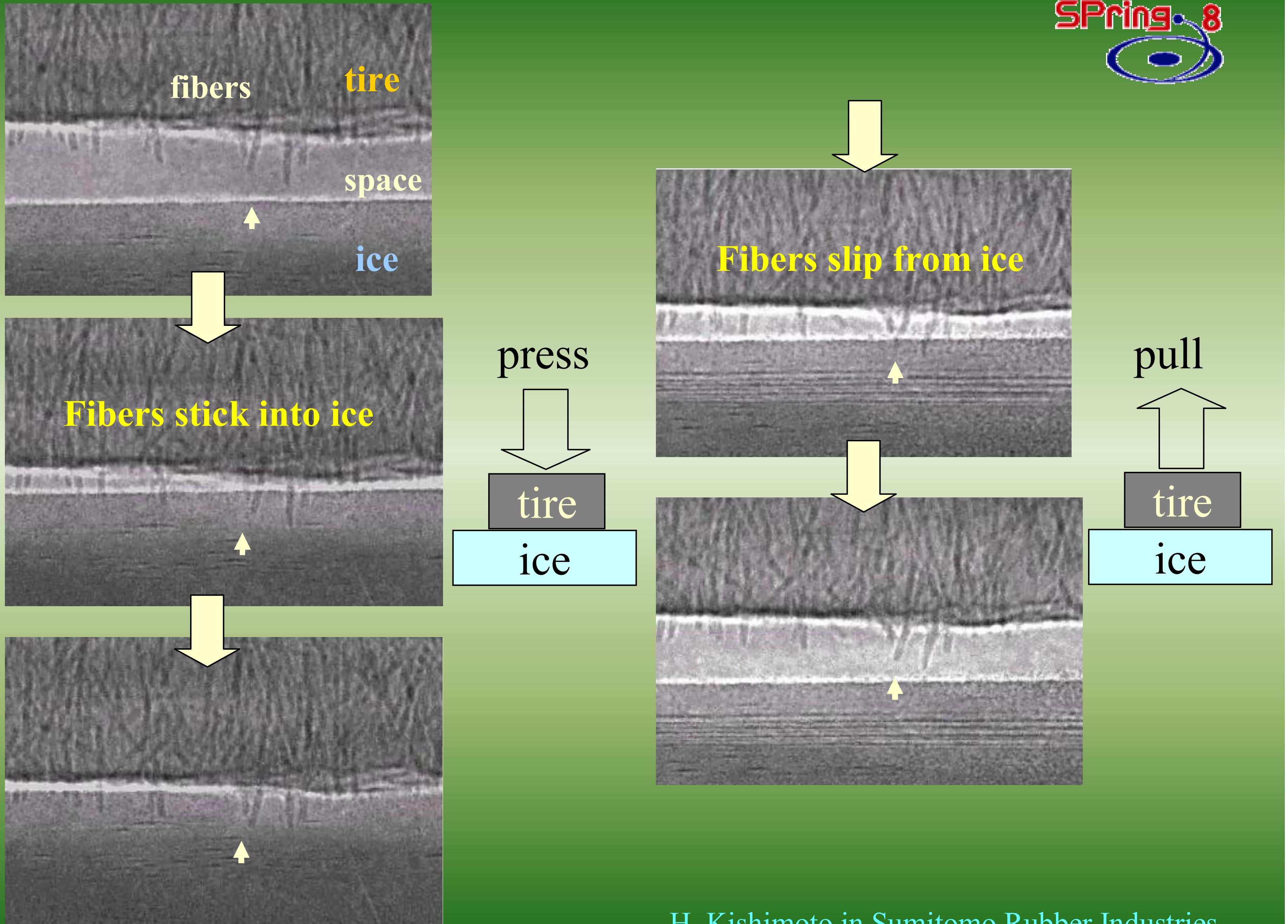

H. Kishimoto in Sumitomo Rubber Industries

Observation of crush of babbles in Al

T. Watanabe in Kobelco Research Institute

Shock absorber for crush

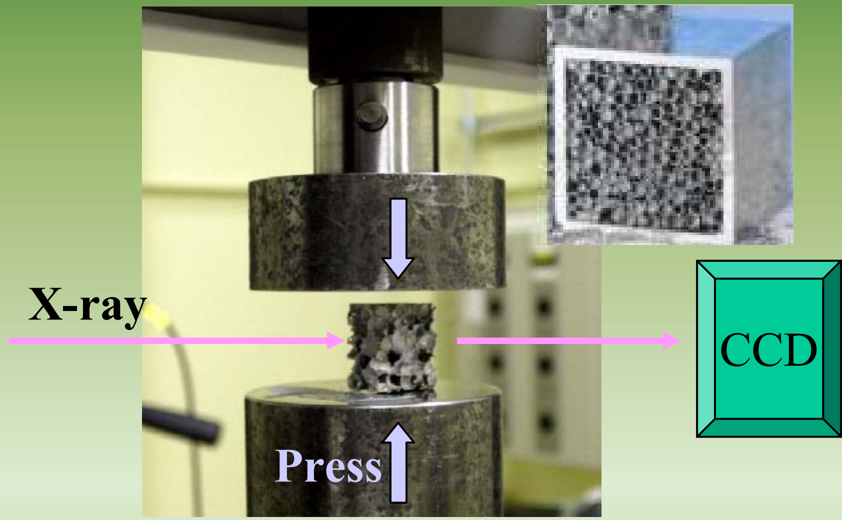

Images stored during 2 sec

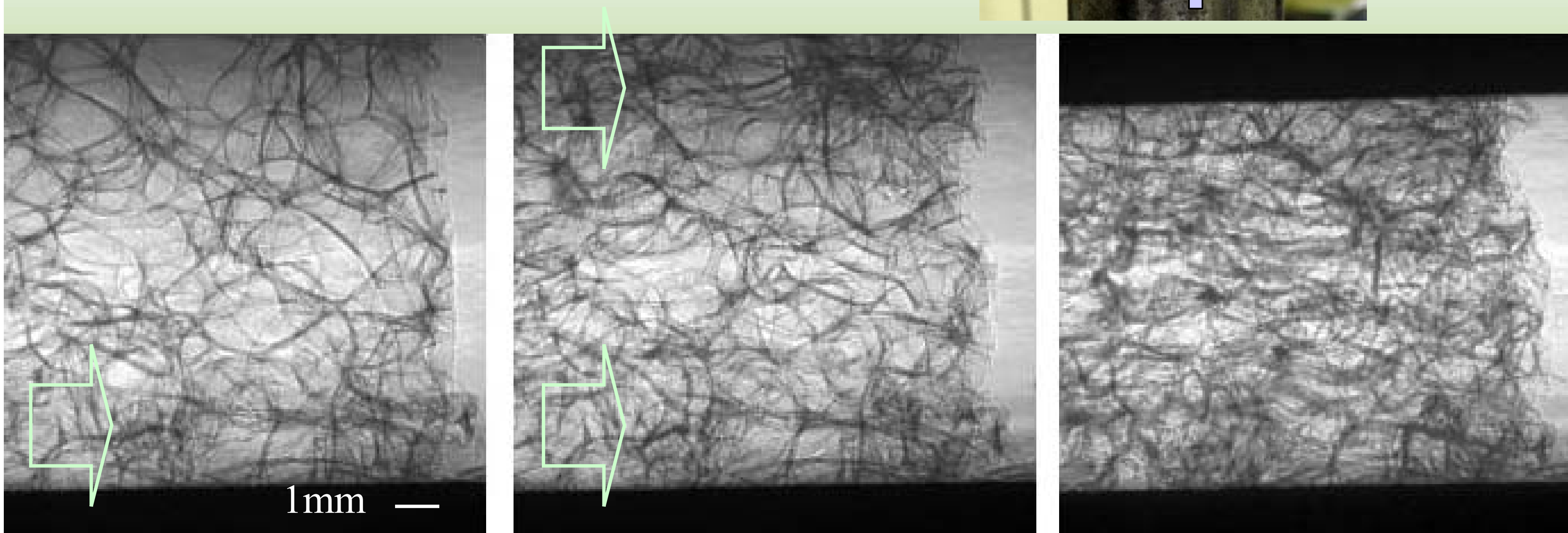

Crush from the bottom side — Crush from the both sides — Crush all

In-situ observation of alloying of galvanized steel by Zn

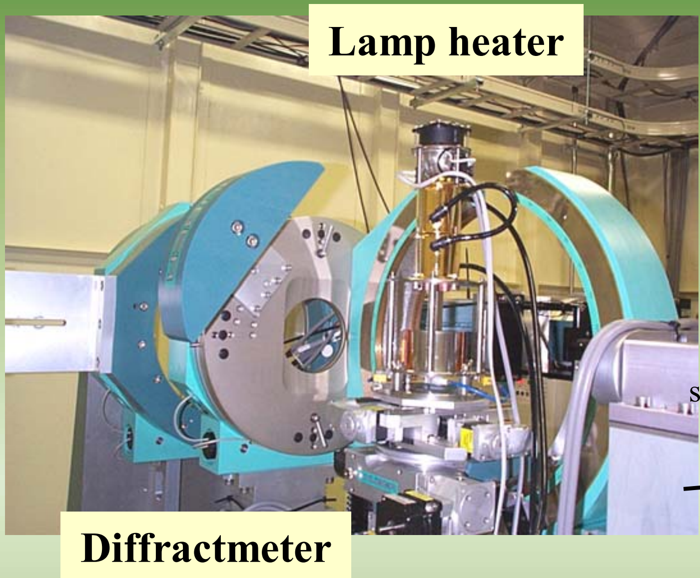

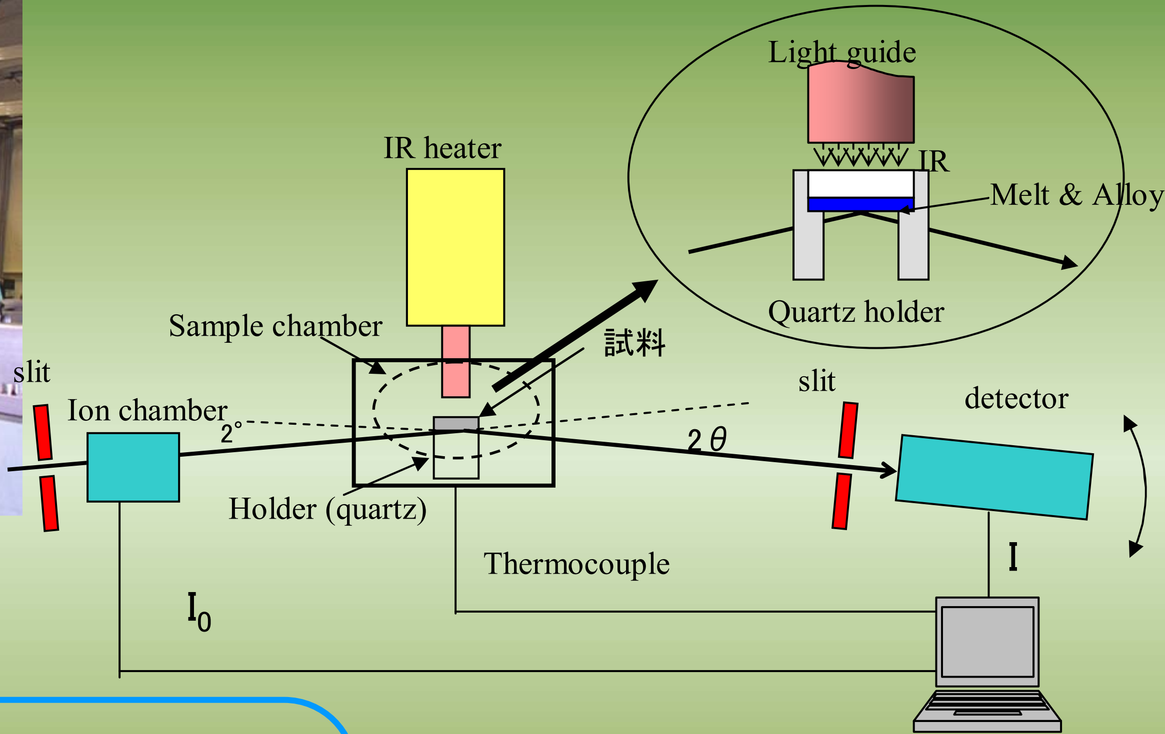

Rust preventive coat

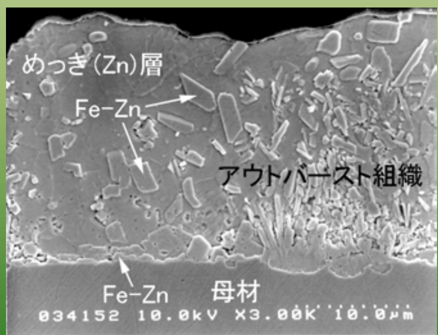

Zn
Fe-Zn alloy
Fe (base)

Alloying process of Zn on steel

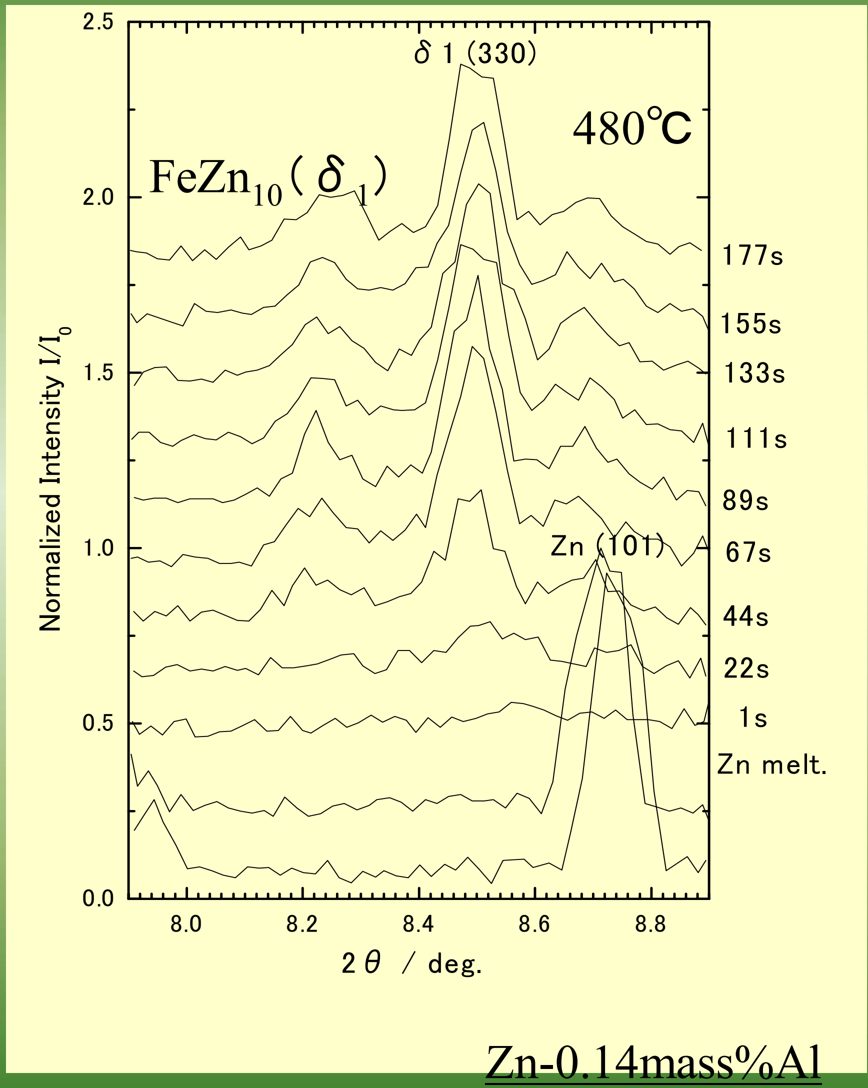

Variation of diffraction profiles on alloying

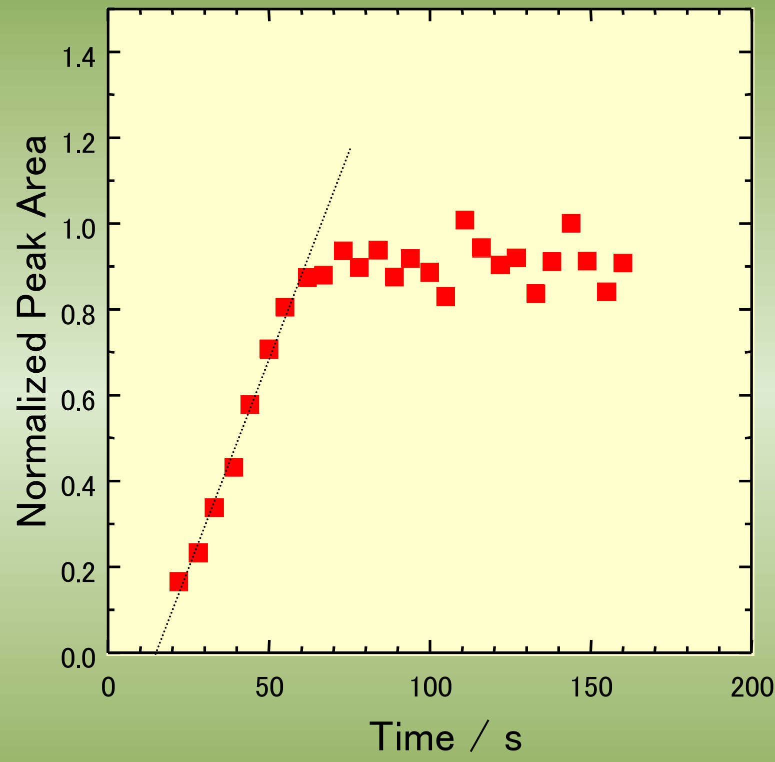

Amount of δ_1 crystals $\propto \sqrt{t}$ (integrated intensities)

⇒ Controlled by diffusion process

A. Taniyama SPring-8 User Experiment Report 2002A0658.

Characterization of inner stress in coats on turbine blades

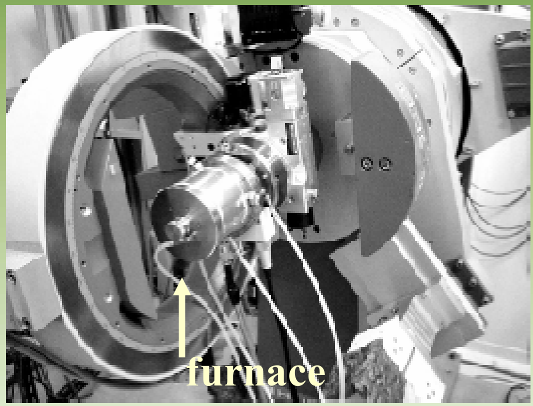

Diffractometer

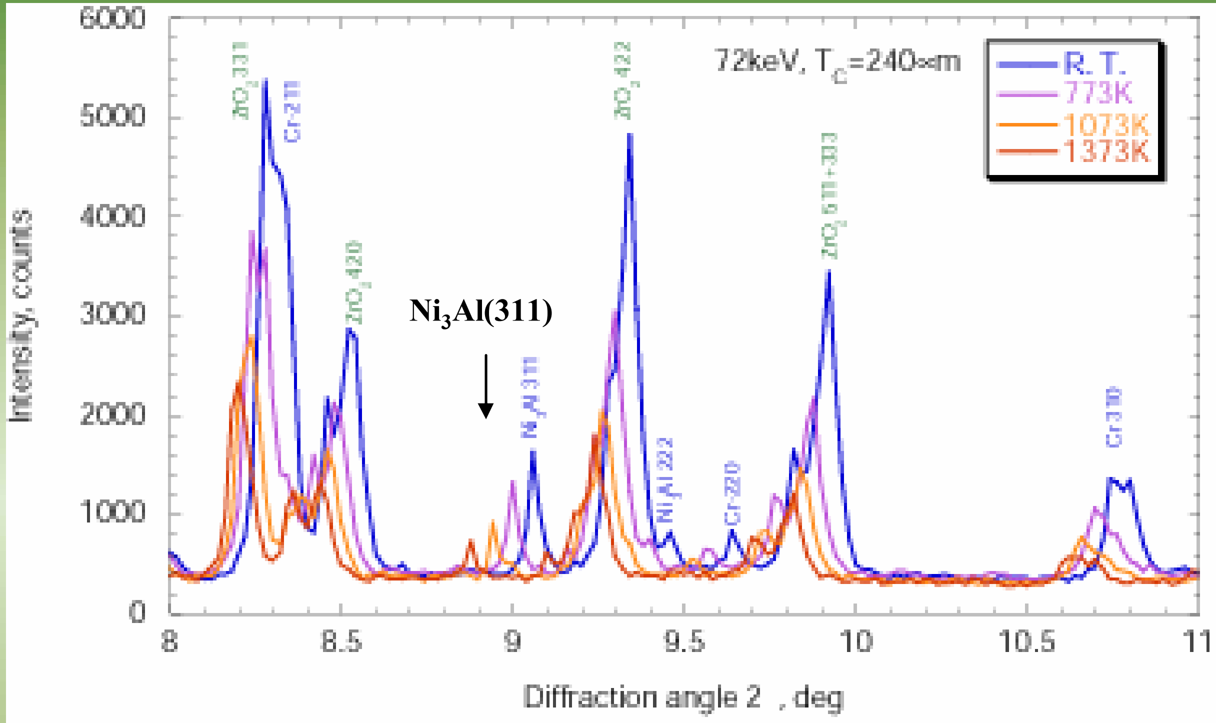

Variation of diffraction profiles on heating

Coat to protect blades from high temperature gas

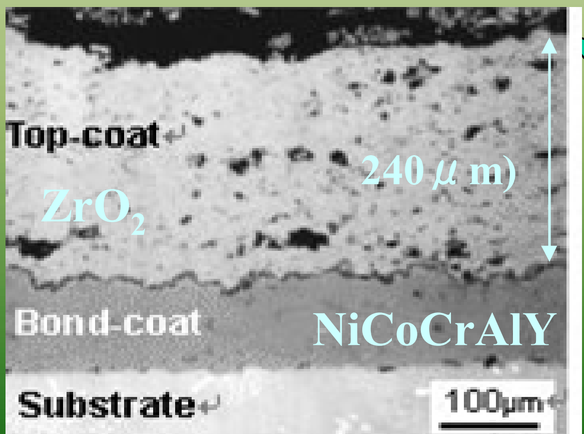

K. Suzuki SPring-8 User Experiment Report No.8 2001B0063.

Temperature dependence of residual stress in bond-coat

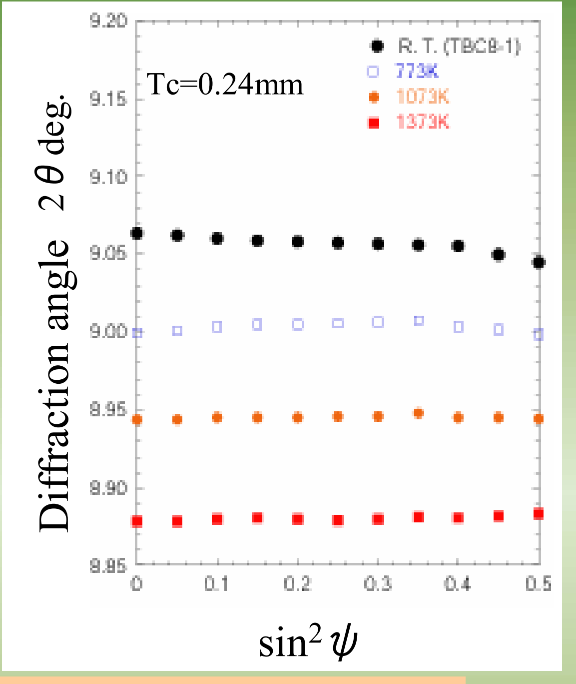

$$2\theta_{\psi} \propto \text{constant} - K\sigma \sin^2\psi$$

$$K = (\tan\theta_0)\,2(1+\nu)/E$$

ν : Poisson's ratio

E : Young's modulaus

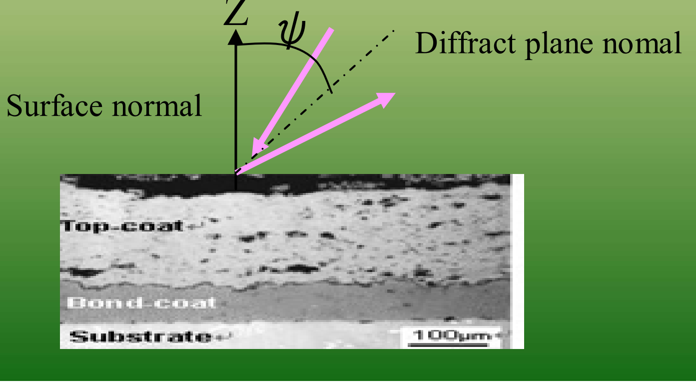

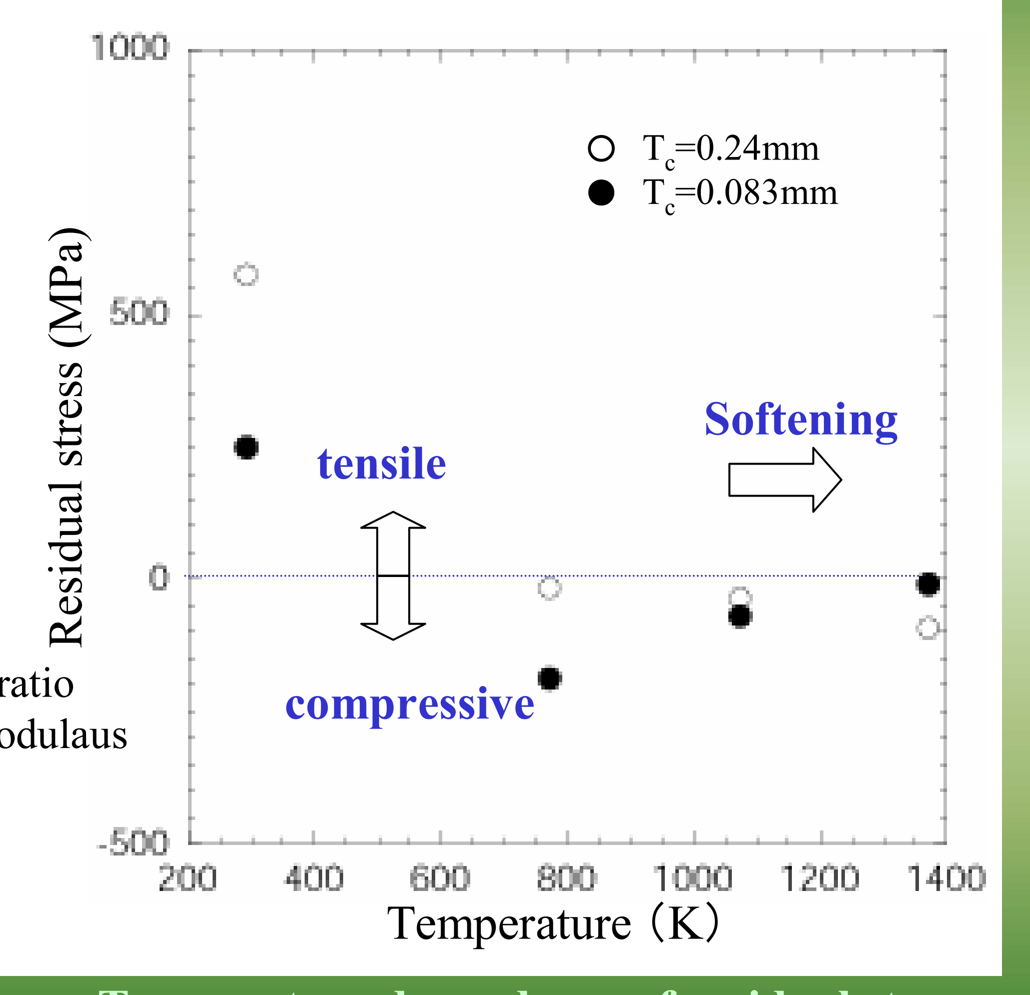

Temperature dependence of residual stress in bond-coat

X-ray micro-beam with zone plate

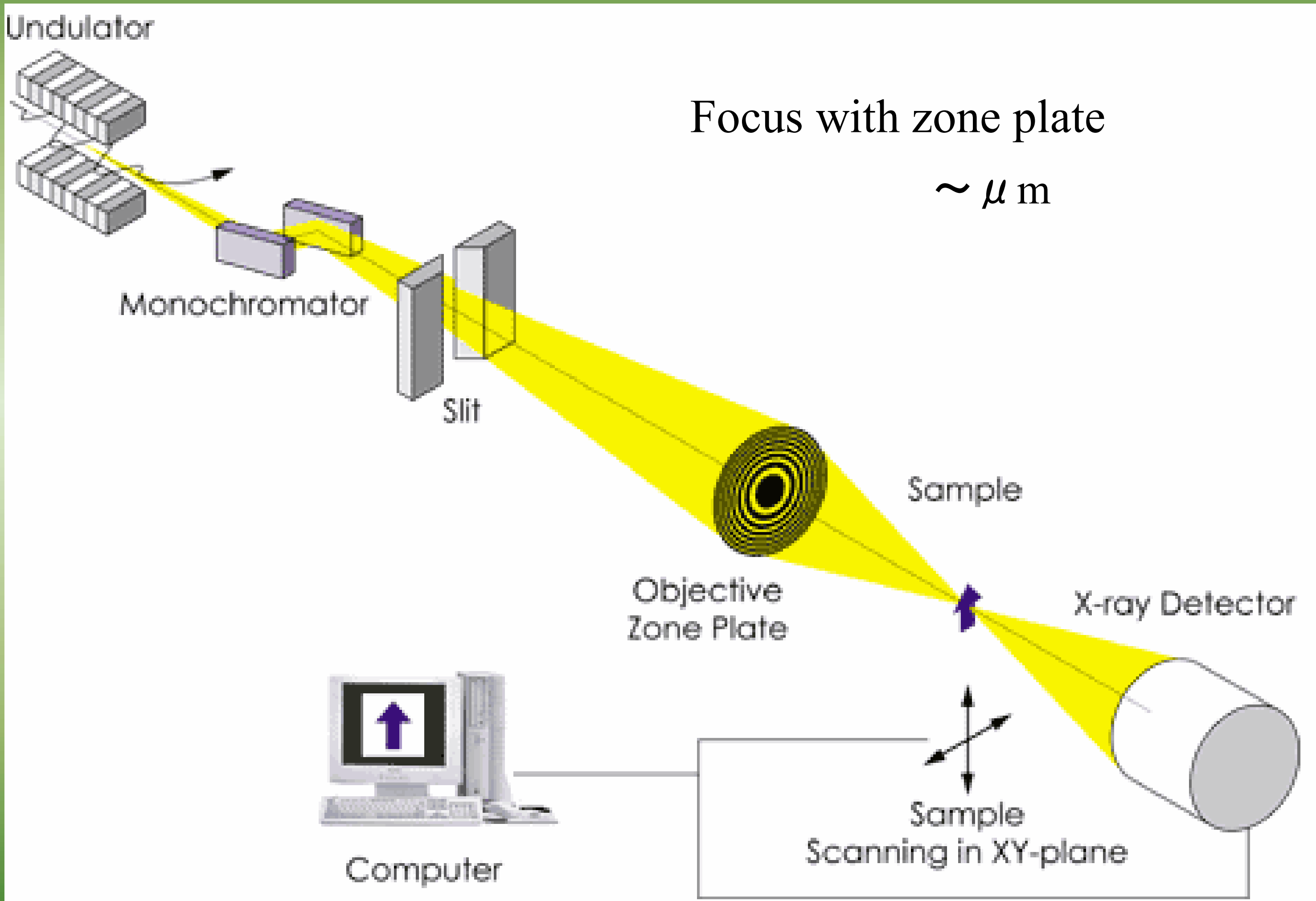

Structural analysis of a single fiber

Structural change at local parts in complex fibers

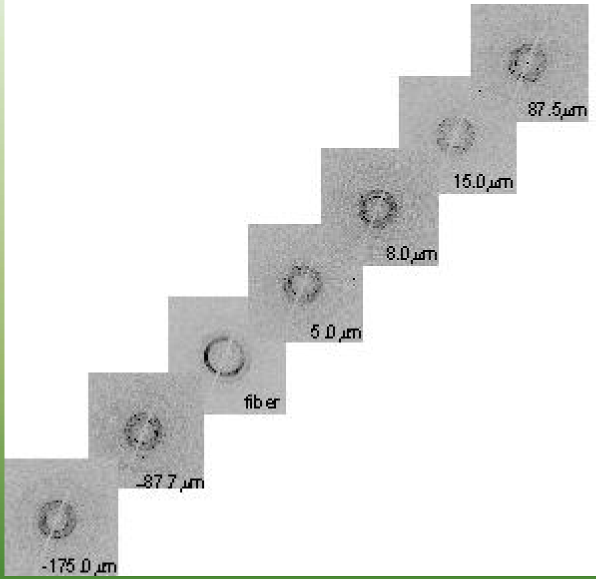

Stress-strain of a PBO single fiber 0.01mm in diameter

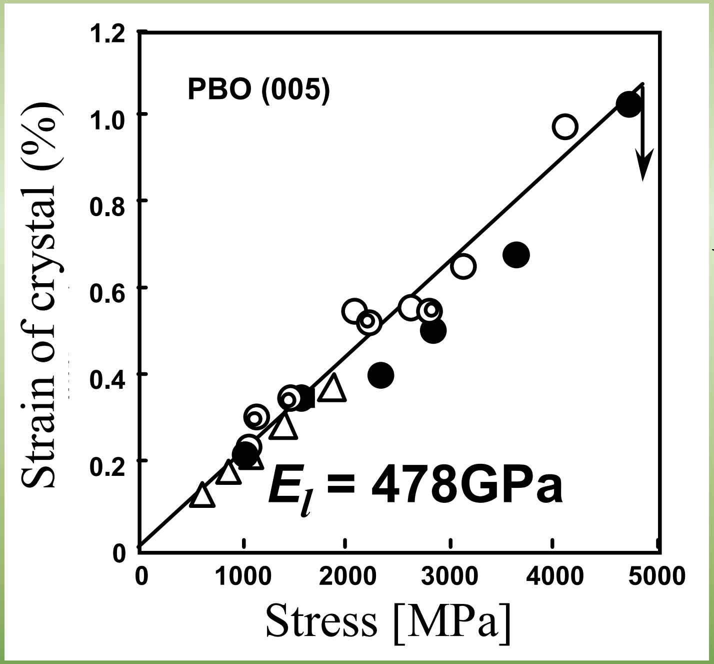

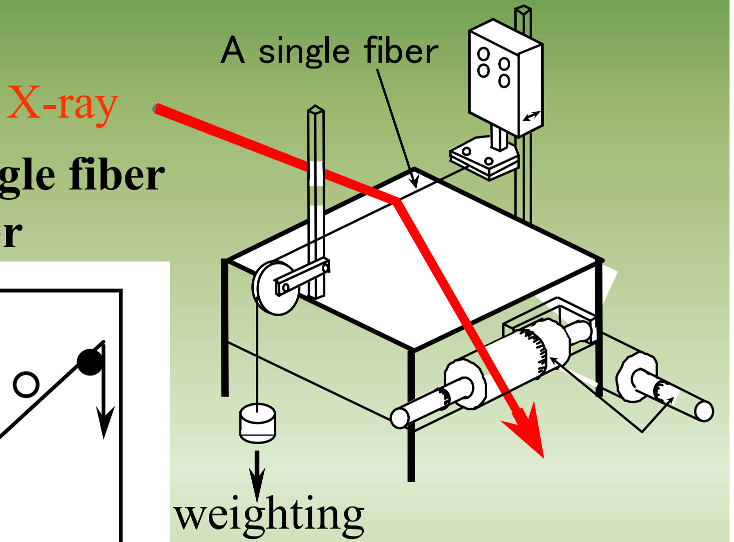

M.Kodera in JASRI

2-D mapping of a very small amount of metals with x-ray fluorescence analysis

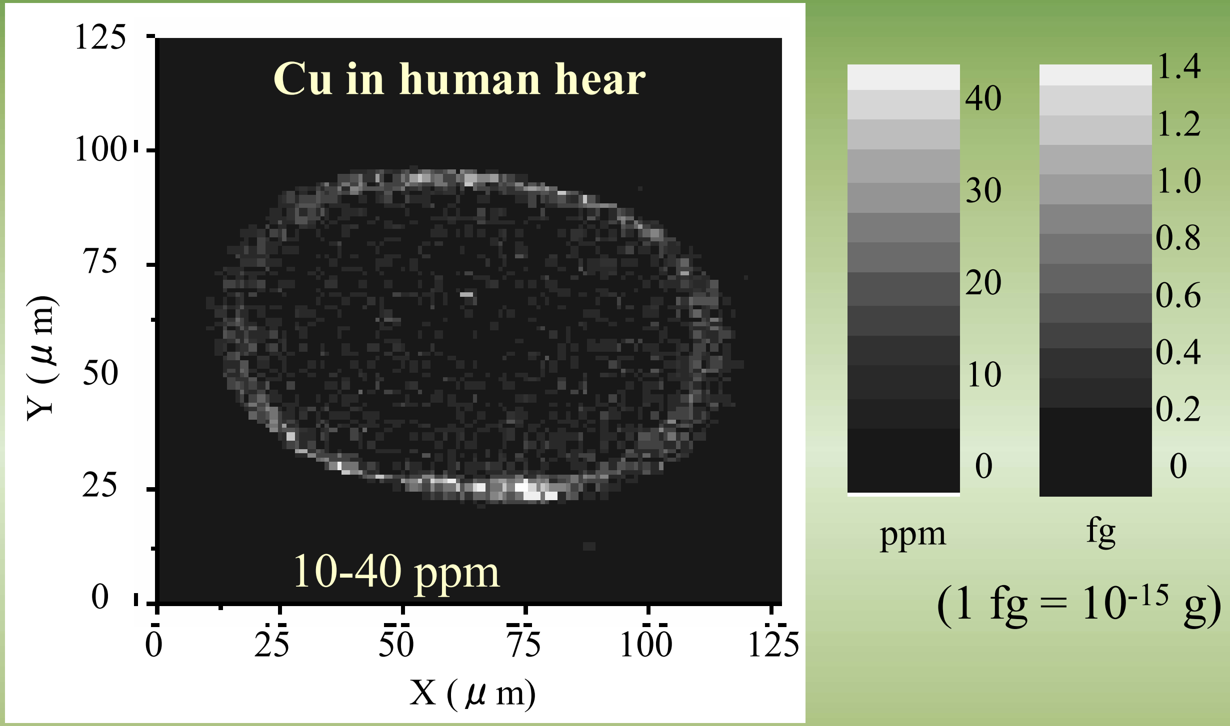

Influence of special water from deep sea on the body

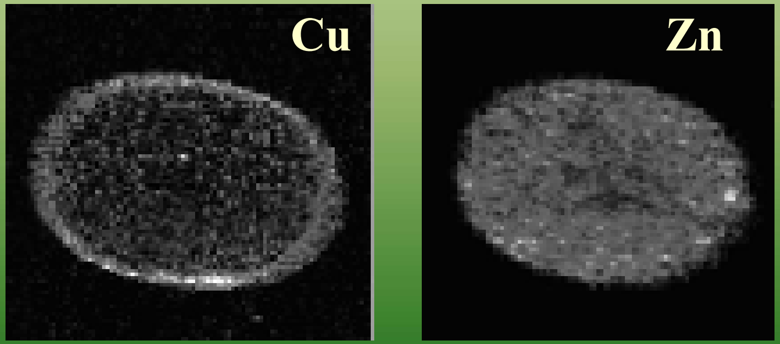

Y.Kagoshima Nucl. Instrum. & Methods. A 467-468 (2001) 872.

Capacity fading on Li ion battery during charge/discharge cycles

—In-situ XAFS study on cathode during cycling of battery—

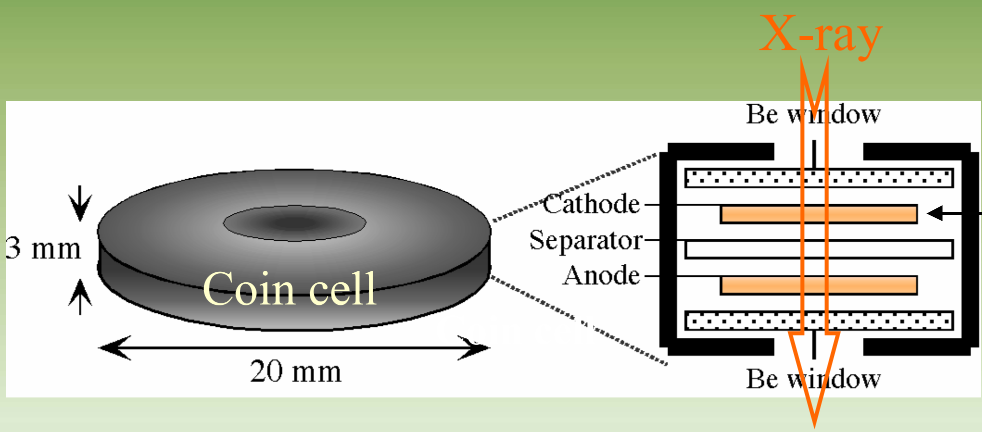

Cathode: $LiNi_{0.8}Co_{0.2}O_2$

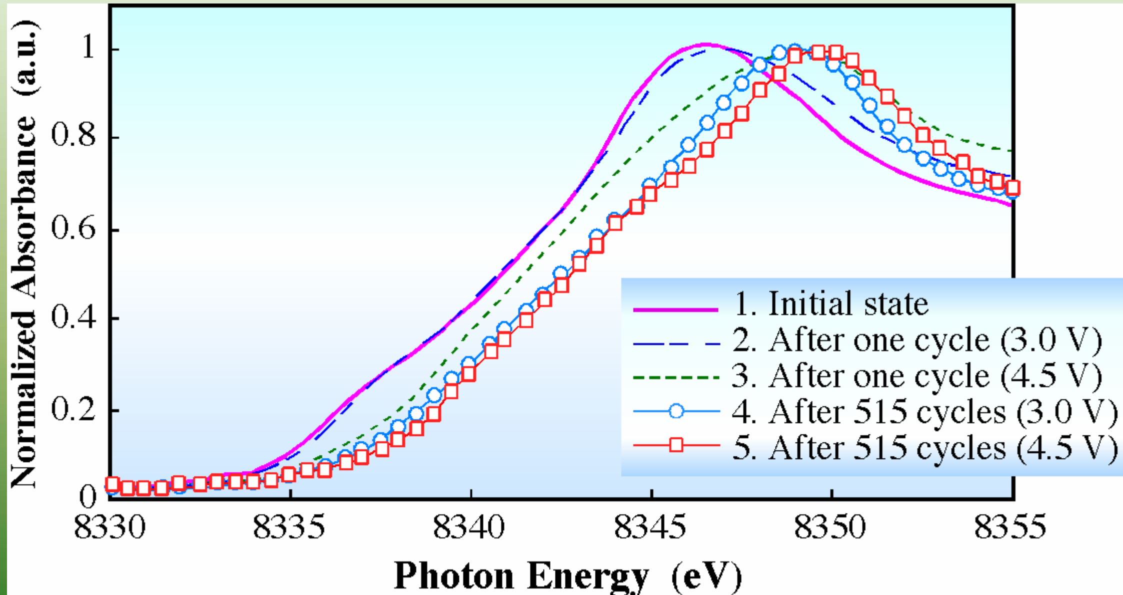

Ni K-edge XANES spectra of $LiNi_{0.8}Co_{0.2}O_2$

Decrease in capacity due to no return of Li into cathode

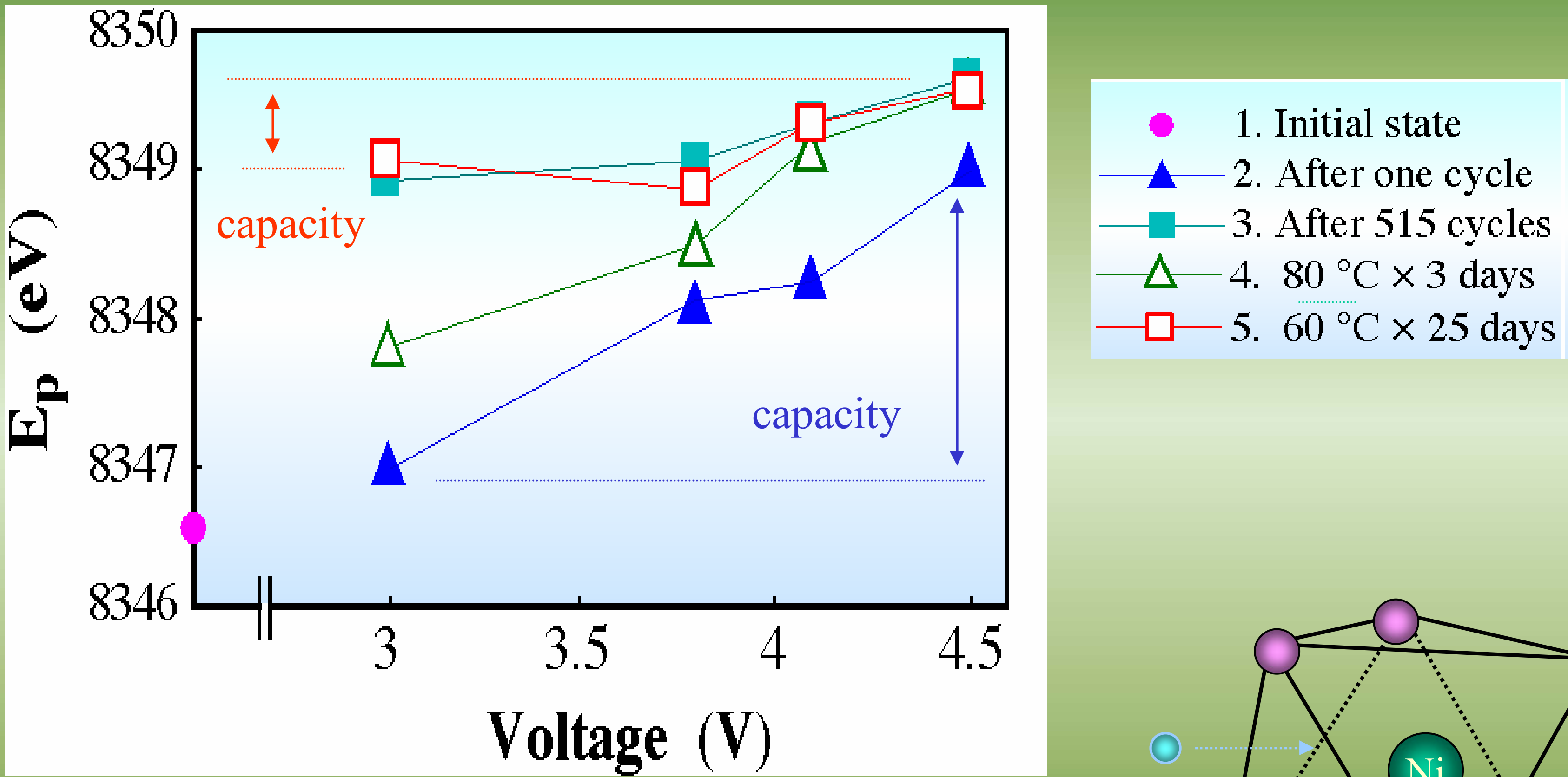

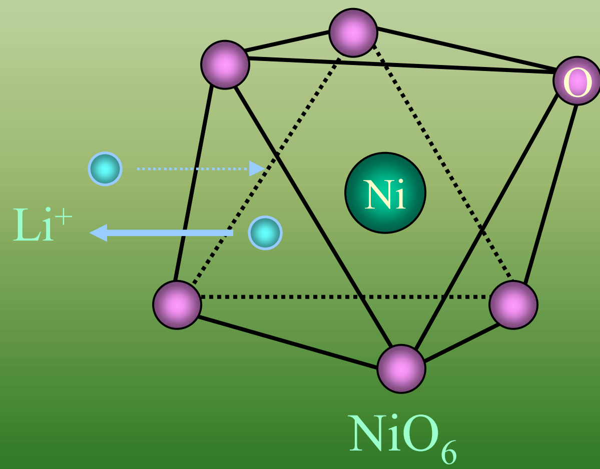

Mechanism of the capacity fading

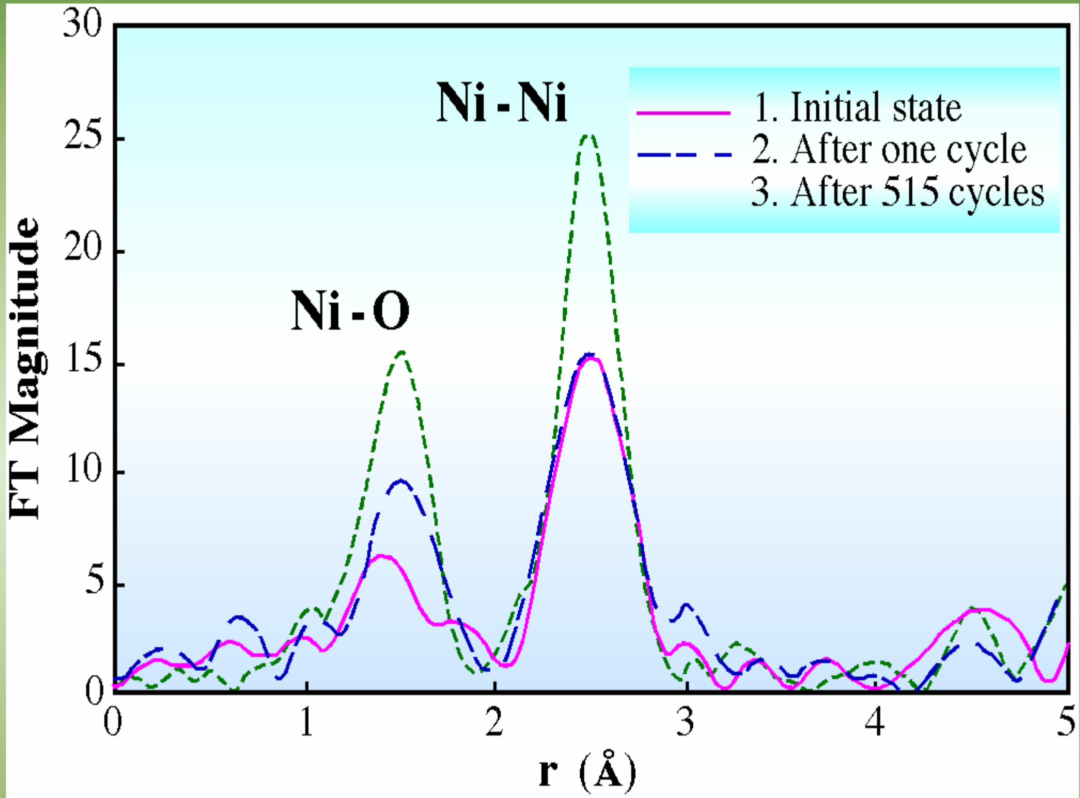

Jahn-Teller distortion

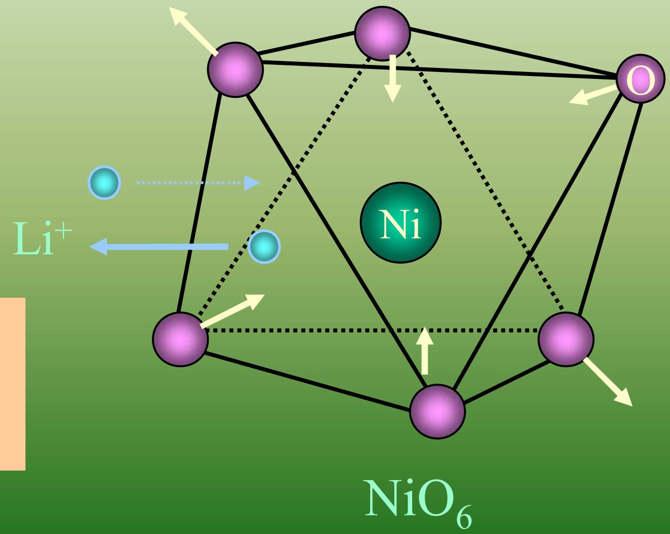

Initial:distorted NiO_6 octahedron
After fading:regular NiO_6 octahedron

T.Nonaka J. Synchrotron rad., 8 (2001) 869.

Request to analysis on material science in industry

- No detectable with other techniques
- How situation : Research, Development, Production
  - R&D : Excellent characterization
  - Development of process : regular measurement according to plan
  - Test : Quality & Quantity & Time
  - Response to trouble : Speed

How can we (SR) reply on request?

Situation in Japan

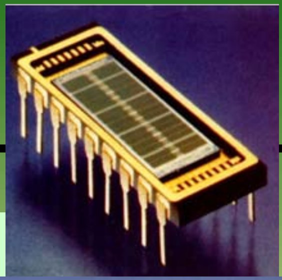

- No detectable with other techniques
- How situation : Research, Development, Production

  - R&D : Excellent characterization

    Structural analysis of thin films of electronic devices

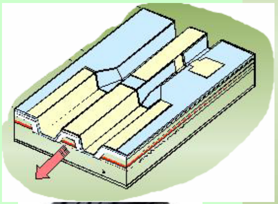

  - Development of process :

    Determination of process conditions for laser

    Imaging of tire and bobbled Al

  - Test : Quality & Quantity & Time

    Not actualized in Japanese facilities

  - Response to trouble : Speed

    No answer

Industrial Applications in Japan

- Films for ULSI, semiconductors
- HDD, DVD
- Semiconductor laser

- Steel & rust preventive coat
- Various coats to prevent heat, stress, etc.
- Al including bubbles

Synchrotron radiation

XAFS, XPS
Diffraction; GIXD, Powder
Reflectivity, Grazing incidence x-ray fluorescence technique
Fluorescence analysis
Imaging, Micro-beam

electronics

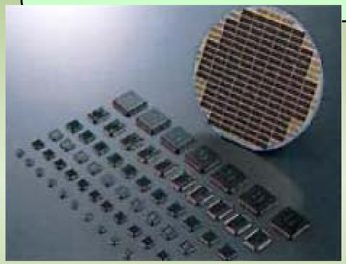

Metals

Soft Materials

- Tires
- Fibers

Others

- Building materials
- Catalysis
- Insects

Energy & Environment

- Batteries: fuel cell & Li-ion
- Analysis of contamination elements
- Catalysts for environment